Geochemical and Sm-Nd isotopic composition of Palaeoproterozoic eclogite and associated rocks in the Usagaran Orogenic Belt, Tanzania

Wing Kei LAU

Tectonics Research and Exploration Group (TRaX)

Department of Geology and Geophysics

University of Adelaide, 5005, Australia

wing.lau@student.adelaide.edu.au

26th October, 2009

Table of Contents

Abstract

Eclogites from the Usagaran Orogenic Belt of Tanzania have been reliably dated at 2.0 Ga and are the oldest reported subduction-related eclogites within a well-preserved orogenic belt. Based on limited geochemistry from two samples of eclogite from the Usagaran Belt, Möller *et al.* (1995) concluded that the protoliths were similar to MORB. This study analyzed a larger number of eclogitic samples and a suite of structurally intercalated mafic and pelitic rocks to establish the tectonic setting of the Usagaran Orogenic Belt rocks.

Eclogitic rocks from the Usagaran Orogenic Belt display LILE and LREE enrichment relative to present-day MORB. Variations in εNd values from depleted mantel at 2.0 Ga supported this interpretation. The mantle-derived mafic rocks show strong Nb depletions, indicating that they are subduction-related. Enrichment of mafic rocks in LILE and LREE are likely caused by dehydration of the subducting slab with some contamination from crustally derived materials perhaps via subducted sediment. The intercalated pelites are mainly derived from the Tanzanian Craton, with a significant mafic input evidenced by high Cr & Ni values. Based on the geochemical isotopic compositions and field relationships, the eclogites, mafic rocks and pelites all formed in a subduction setting that operated around 2.0 Ga.

Despite the fact that the Earth was hotter in its early history, modern plate tectonics, (i. e., subduction of cold oceanic crust into a warm mantle resulting in high-pressure low-temperature metamorphism), occurred and was recorded in the Usagaran Belt during the Palaeoproterozoic. Thus modern-style plate tectonics have operated since at least 2.0 Ga.

1. Introduction

Eclogitic facies rocks form under high to ultra-high pressure metamorphic conditions (Blatt and Tracy, 1996). Some eclogites are thought to occur at the uppermost lithospheric mantle in both sub-continental and sub-oceanic regions and are brought near to the surface as xenoliths by intra-plate alkali basalt or kimberlite eruption (Blatt and Tracy, 1996). Eclogite can also form when mafic rocks are subjected to high-pressure moderate-temperature metamorphism where the minimum P-T condition is about 14kbar (50 km) and 450°C (Blatt and Tracy, 1996). These conditions can be met in subduction-accretion complexes and sites of continental collisions in modern Earth, where relatively cold crust is subducted deep into the mantle, then exhumed back to the Earth's surface before the eclogitic mineral assemblages are overprinted as the tectonic depressed isotherms re-equilibrate. Such eclogites are the remnants of tectonic crustal-thickening processes and are considered to be the evidence of former subduction zones (Möller *et al.*, 1995).

Studies of subduction-related eclogites are important because they retain information about the tectonic process involved in their formation. Thus the study of eclogites can improve our understanding of how tectonic processes operated in the past.

Subduction-related eclogites are relatively common in Phanerozoic orogens (Brown, 2007), e.g., 445 Ma eclogites from North Qaidam, northwest China, (Zhang *et al.*, 2008); 230 Ma eclogite from western Tianshan orogenic belt, China, (Zhang *et al.*, 2007); 100 Ma eclogites from Pohorje Mountain of the Eastern Alps, Northern Slovenia (Sassi *et al.*, 2004).

On the other hand, few Precambrian eclogites are reported (Brown, 2007). Examples include the 620 Ma Mali ultrahigh-pressure (UHP) eclogites (Jahn *et al.*, 2001); 1.9 Ga eclogite from the Snowbird Tectonic Zone, Canada (Baldwin *et al.*, 2004); the 2.0 Ga eclogites from the Usagaran Orogenic Belt, Tanzania (Möller *et al.*, 1995; Collins *et al.*, 2004) and the 2.7 Ga eclogites from the Belomorian region of NW Russia (Volodichev *et al.*, 2004). Of these, only eclogites from the Usagaran have been reliably dated at 2.0 Ga

(Möller *et al.*, 1995; Collins *et al.*, 2004) and are the oldest reported subduction-related eclogites within a well-preserved orogenic belt.

Oceanic crust is partly made of mid-oceanic ridge basalt (MORB). MORB is a type of tholeiitic basalt that erupts along the mid-ocean ridges on constructive-plate margins. Oceanic crust gradually migrates from its source of formation towards the destructive-plate margins and then subducts into the mantle. Eclogites with MORB affinity represent former oceanic crusts that have experienced all stages of plate tectonics and hence, they are the best evidence of plate tectonics.

Different workers apply different distinctive features of plate tectonics to define and trace its operations back in time. For example, Cawood *et al.* (2006) suggest that plate tectonics have been active since at least 3.1 Ga based on palaeomagnetic, geochemical and tectonostratigraphic data while Stern (2005) thinks the first appearance of ophiolites, blueschist facies metamorphic rocks and ultrahigh-pressure metamorphic terranes indicate that modern style of subduction tectonics began in the Neoproterozoic. Although different lines of evidence show that plate tectonics initiated in the Precambrian, there is still debate on when exactly it started. The definition of plate tectonics used in this study is based on the fact that old cold oceanic crust subducts into warm mantle beneath the subduction zone. Eclogitic rocks are then the products of these high-pressure low-temperature conditions. This type of tectonic operation is common in the recent history of the Earth (since at least the Phanerozoic) and hence, it is named as 'modern plate tectonics'. Discovery of 2.0 Ga old subduction-related eclogites with MORB affinity is remarkable as it indicates a more precise possible timing of the onset of modern plate tectonics.

Based on limited geochemistry from two samples of eclogites from the Usagaran Orogenic Belt, Möller *et al.* (1995) concluded that the protoliths were similar to MORB. This study aims to investigate whether the eclogites from the Usagaran Orogenic Belt truly have MORB affinity by analyzing a larger number of eclogitic samples and a suite of structurally inter-related mafic and pelitic rocks for their bulk-rock geochemistry and Sm-Nd isotopic compositions. Possible tectonics setting(s) will be proposed based on the results.

2. Geological Setting

The Usagaran Orogenic Belt, situated in central Tanzania, is a Palaeoproterozoic orogenic belt that lies directly east of the Late Archaean Tanzanian Craton (Figure 1). In the south it has been linked with a similar sequence of rocks of the Ubendian Orogenic Belt of western Tanzania (Mruma, 1989). The Usagaran Orogenic Belt is progressively reworked in the north and east by the East African Orogen, a Neoproterozoic orogeny associated with the amalgamation of Gondwana (Collins *et al.*, 2004).

The Usagaran Orogenic Belt can be subdivided into two major litho-tectonic units: the Konse Group and the Isimani Suite (Mruma, 1980; Reddy *et al.*, 2003, Collins *et al.*, 2004, Reddy *et al.*, 2004). The Isimani Suite is composed of medium to high grade gneisses and amphibolites with a few pockets of granulites (Mruma, 1989). The rocks of the suite have undergone high-grade metamorphism at amphibolite- to granulite-facies, have been multiply deformed and have completely transposed primary structures (Mruma, 1989). The eclogites and the mafic rocks occur as lenses in the garnet amphibolites, together with metapelites and felsic gneisses in the Isimani Suite (Collins *et al.*, 2004; Brick, personal communication). The Konse Group is bordered by the Tanzanian Craton and by the Isimani Suite to the west and east respectively (Mruma, 1989). It is composed of six low-grade meta-sedimentary and meta-volcanic formations which still show their primary sedimentary and volcanic structures (Mruma, 1989).

The contacts between the Isimani Suite and Konse Group are mainly tectonic, defined by prominent thrust planes and mylonite zones with the Isimani Suite overthrust onto the Konse Group (Mruma, 1989). However, the Isimani suite is overlain by the Konse Group with a well marked angular unconformity in some areas (Mruma, 1989). The contacts between the Konse Group and the Tanzanian Craton are tectonic as the Konse Group has been thrust onto the craton (Mruma, 1989).

There are at least two major metamorphic events can be recognized in the Isimani Suite, whereas the Konse Group displays one episode of metamorphic recrystallization (Mruma, 1989). The Isimani Suite was first metamorphosed to granulite to upper amphibolite conditions (T = 780ºC and P = 10 kbars) and then retrograded to green

schist – amphibolite facies (T = 500ºC to 700ºC and P = 4 kbar to 6 kbar) (Mruma, 1989). The Konse Group was metamorphosed under the conditions similar to the retrograded metamorphism in the Isimani Suite (Mruma, 1989).

Peak eclogite-facies conditions have been constrained at 750°C and about 18 kbar (Möller *et al.*, 1995). A clockwise P-T path is deduced from mineral zonation and inclusion relations (Möller *et al.*, 1995). Retrograde reaction textures indicate a near-isothermal decompression which can be explained by erosion or tectonically controlled exhumation that followed tectonic thickening of the crust during subduction (Möller *et al.*, 1995). These findings are supported by Herms' (2002) investigation on fluid inclusions associated with the eclogitic rocks.

The Isimani Suite of the Usagaran Orogenic Belt records a complex structural history which can be summarized in five stages (Reddy *et al.*, 2003). The initial stage (D_1) occurred at high pressure conditions and resulted in formation of recumbent folds and compositional bandings (Mruma, 1989; Reddy *et al.*, 2003). The eclogite and granulite facies mineral assemblages are considered to have developed at this stage (Mruma, 1989). The second stage (D_2) took place at amphibolite facies conditions and overprinted the previous D_1 deformations as well as mineral assemblages (Reddy *et al.*, 2003). The third stage (D_3) was short-lived and the metamorphic grade of the D_3 fabrics are indistinguishable from those developed during D_2 which indicates that it was probably associated with the later stages of D_2 (Reddy *et al.*, 2003). D_3 may represent a phase when the direction of shortening changed from SE to S during the orogeny (Reddy *et al.*, 2003). The last two stages involved extension (D_4) followed by thrusting (D_5) under greenschist facies condition that thrust the Isimani Suite over the Konse Group (Reddy *et al.*, 2003). The ages of the D_4 and D_5 deformation phases are poorly constrained and may reflect deformation during Palaeoproterozoic exhumation of the Usagaran Orogen or during the late Neoproterozoic East African orogeny (Reddy *et al.*, 2003).

There are a number of published works constraining the nature and age of protoliths, timing of deformation and metamorphism within the Usagaran Orogenic Belt by using geochronological data and isotopes studies (Möller *et al.*, 1995; Herms, 2002; Collins *et al.*, 2004). Nd-model ages from the Usagaran gneisses range between 2.7 – 3.1 Ga,

suggests that there were some Achaean component (Möller *et al.*, 1998). Similar results were obtained from the U-Pb study on the zircon cores from pelites by using sensitive high resolution ion microprobe (SHRIMP) (Reddy *et al.*, 2003). U-Pb analysis of monazite and rutile from metapelitic rocks suggest that the eclogite facies metamorphism took place at about 2 Ga (Möller *et al.*, 1995), similar to the SHRIMP U-Pb zircon ages obtained from the eclogite by Collins *et al.* (2004). The area was then affected by an extensive amphibolite facies metamorphism which took place between 1.87 – 2.0 Ga (Reddy *et al.*, 2003).

3. Sample selection & analytical methods

Twenty rock samples including nine eclogitic rocks, six mafic rocks and five metapelites, were analyzed for major and trace element composition. Samples were selected to provide the widest possible sample spacing within the eclogite and mafic rock body, and pelites most closely associated with the eclogites (figure 1b). Weathered parts of the samples were removed by hammer before they were crushed in a steel jaw crusher and milled to powder by a tungsten-carbide mill at the University of Adelaide. The rock powders were sent to Amdel Limited, Thebarton, South Australia, for major and trace elements analysis. The major elements and trace elements were analyzed by inductively coupled plasma optical emission spectrometry (ICP-OES) and inductively coupled plasma elemental mass spectrometry (ICP-EMS) respectively. The results, with additional two mafic samples (T06-38 and T06-39) previously analyzed by ALS, are reported in Table 1. Note that sample T06-39 has been analyzed twice and the results are comparable.

Ten out of these twenty samples, including five eclogitic rocks, three mafic rocks and two pelites, were selected for Sm-Nd isotopic compositions analysis. Sample preparation and isotopic analyses were undertaken in the University of Adelaide isotope laboratory. Sm-Nd isotope analytical procedure followed that outlined in Wade *et al.* (2006). Powdered samples were spiked with a mixed ^{149}Sm-^{150}Nd spike before oven digestion in sealed Teflon steel bombs. Sm and Nd were separated from other trace elements by two stages of dilute hydrochloric acid cation exchange. The two elements were then separated by hydrogen-diethyl-hexyl-phosphate reverse chromatography

procedure. The products were then analyzed by thermal ionization mass spectrometers (TIMS). Nd analyses were carried out on a Finnigan MAT 262 multi-collector mass spectrometer in dynamic mode while Sm analyses were carried out on a Finnegan MAT 261 single-collector mass spectrometer. Analyses of the La Jolla standard yielded 0.511839 ± 0.000005 (1 SD) on 12 runs during the course of the study. The calculated results are listed in Table 2.

4. Petrology

The mineral assemblages of the eclogites consist of garnet, clinopyroxene and a small amount of quartz. Presence of plagioclase, amphiboles and ilmenite are due to retrograde metamorphism to the amphibolites facies. In the sample with least evidence of retrogression (T01-40), garnet and clinopyroxene are similar in size and have a granoblastic texture. Some garnets are surrounded by plagioclase and quartz while some clinopyroxene grains are surrounded or replaced by amphiboles (Figure 2a & 2b). Cleavages of clinopyroxene are slightly faded out and ilmenites are found along them or as patches next to clinopyroxene. Some thin sections have porphyroblastic garnets within a matrix of finer-grained plagioclase, clinopyroxene, ilmenite, quartz and amphibole. Some eclogitic rocks also show a weak foliation defined by an alignment of clinopyroxene, amphibole and vein quartz penetrations (Figure 2c & 2d), probably formed after eclogitic metamorphism.

The mafic rocks consist of orthopyroxene, clinopyroxene, plagioclase, olivine and minor quartz. Similar to the eclogitic rocks, some pyroxenes are broken down to form amphiboles and ilmenite although some pyroxenes generally have well preserved crystal shapes and cleavages (Figure 2e & 2f). These indicate that the rocks are only slightly metamorphosed to amphibolites facies. Garnet forms a reaction rim between plagioclase and orthopyroxene in thin section T06-38 (Figure 2g & 2h). This assemblage shows a reaction between plagioclase and orthopyroxene to form garnet, which is common from medium-amphibolites facies or hotter metamorphism. Furthermore, small amount of scapolite are found in mafic sample T06-39.

5. Results

5.1 Whole rock major and trace element chemistry

5.1.1 Eclogite

The major element concentrations of the eclogitic samples are broadly similar with the exception of sample T07-16, which is penetrated by vein quartz. Therefore, it is excluded from major and trace elements classification plots, but its spidergram and REE pattern will be kept for comparisons in order to demonstrate the effect of fluid alteration on distribution of trace elements.

The eclogitic rocks have low SiO_2 contents which vary from 47.5 to 52.1%, a typical range of basic rocks. As the eclogitic rocks have low silica and low total alkali content, they plot in the basalt field in the total alkalis-silica (TAS) diagram (Figure 3a) and in the tholeiite field on an AFM diagram (Figure 3b). This is also shown by the P_2O_5-Zr discrimination diagram (Figure 3c) as alkali basalt has higher P_2O_5 than tholeiitic basalt for a given Zr content (Winchester and Floyd, 1976). Their low MgO, Cr, Ni content and high CaO as well as FeO_{total} concentrations indicate they probably have a primitive basic protolith. Similar conclusions are obtained from the Al_2O_3-TiO_2 discrimination diagram (Figure 3d) generated by Pearce (1983) and applied by Miller and Thöni (1997) as well as Sassi *et al.* (2004) to distinguish between cumulates and basalts. The diagram shows the eclogitic rocks represent basaltic liquid compositions. Furthermore, the eclogitic rocks are generally characterized by low loss of ignition (LOI) contents, indicating that fluid phases were not significantly involved during subduction, exhumation and post-metamorphism.

The E-MORB-normalized spidergram shows the eclogitic rocks are enriched in Ba as well as U while depleted in Rb, K and Sr (Figure 4b). The trace elements abundances vary from 0.2 to 10 times to E-MORB while most of the rare earth elements (REE) concentrations fluctuate between 0.4 to 3 times to E-MORB. Sample T07-16 has the same spidergram pattern as the others but generally lower in concentration. Strong depletions are found in Nb and Sr. In addition, its REE pattern remains the same as the other samples.

All eclogitic samples plot in the oceanic tholeiite field in the TiO_2-K_2O-P_2O_5 discrimination diagram (Figure 6c). Most of the eclogitic rocks are classified as MORB in various discrimination diagrams, such as the Ti-Zr-Y discrimination diagram (Figure 6a), the Ti-Zr discrimination diagram (Figure 6b), the Zr-Nb-Y discrimination diagram (Figure 6d) and the Ti-V discrimination diagram (Figure 6e). The exceptions are sample T07-06 which is classified as island-arc tholeiites in the Ti-Zr discrimination diagram and two samples (T07-06 and T07-24) fall into the island arc basalt or continental arc in the Ti-V discrimination diagram.

The total REE concentrations of the eclogitic rocks varied between 33.73 to 63.7 ppm, with sample T06-11 showing the most significant REE enrichment at 119.25 ppm. The $(La/Sm)_N$ range from 0.62 to 2.34 while $(La/Yb)_N$ varies between 0.89 – 2.73, indicating a light rare earth element (LREE) enrichment. The REE concentrations are 10 to 45 times to chondrite concentrations (Figure 4c). Note that LREE concentrations of sample T06-11 are up to 65 times to chondrite. There are no significant Eu anomalies among the samples. The total REE concentration of T07-16 is 39.93 ppm. Its REE pattern follows the same trend as the others but is lower in concentration, with $(La/Sm)_N$ and $(La/Yb)_N$ equal to 1.38 and 2.69 respectively.

5.1.2 Mafic rocks

As with the eclogitic rocks, the mafic rocks show very uniform major element concentrations with only limited variations. The mafic rocks lie on the boundary between basalt and basaltic andesites in the TAS diagram (Figure 3a). They fall into the tholeiitic field in an AFM diagram (Figure 3b) and the P_2O_5-Zr discrimination diagram (Figure 3c). Al_2O_3-TiO_2 discrimination diagram indicates that the mafic rocks are cumulates (Figure 3d), though no Eu anomalies are seen in the chondrite normalized REE plot (Figure 5b). They have low LOI content with an average about 0.2 %, indicating that no significant volatile fluid phase was involved during their formation and metamorphism.

The primitive mantle-normalized spidergram of the mafic rocks (Figure 5a) shows a gradual decreasing trend in concentrations from the most incompatible element to the least incompatible element. All samples are strongly depleted in Nb while only slight depletions are found in Ti. The trace elements abundances vary from 2 to 40 times to

primitive mantle except Nb concentrations which are generally equal to the primitive mantle value.

The mafic rock samples are plotted in the continental tholeiite field in the TiO_2-K_2O-P_2O_5 discrimination diagram (Figure 6c). However, they fall along the boundaries of field B, C and D in the Ti-Zr-Y discrimination diagram (Figure 6a). They are classified as arc basalts in the Ti-V discrimination diagram (Figure 6e).

The mafic rocks have different REE patterns from the eclogitic rocks. The total REE concentrations of the mafic rocks vary from 40.52 to 58.02 ppm. Abundances of trace elements vary from 4 to 45 times to chondrite. Similar to the primitive mantle-normalized spidergram, the chondrite-normalized REE patterns of the mafic rocks (figure 5b) show a gradual decreasing trend in abundance from La to Lu. Ratios of $(La/Sm)_N$ and $(La/Yb)_N$ range 2.44 – 2.74 and 5.91 – 7.17 respectively.

5.1.3 Pelite

The SiO_2 content of sample T06-07 is 35.9%. Its MgO concentration and LOI are anomalously high at 17.1% and 8.62%. Therefore, it is probably a dolomite with some detrital material. Other pelitic samples have SiO_2 range between 54.3 – 60.1%, with relatively high Al_2O_3 content (17.1 – 26.4 %). The protolith of the pelites were probably shale. Cr and Ni abundances are 385 – 650 ppm and 70 – 175 ppm respectively. The total REE concentrations of the pelite varied range between 126.98 ppm – 194.02 ppm. The HREE is slightly enriched relative to the LREE according to the Post-Archaean average Australian sedimentary rock (PAAS) normalized REE plots (Figure 5c). However, no significant Eu anomaly is observed.

The lack of Eu anomaly suggests that the majority of the sediments are derived from an Archaean source. This is also supported by the zircon ages obtained from samples T01-05 (Collins *et al.*, 2004). The zircon cores from sample T01-05 range from 2400 to 3000 Ma and two large peaks are found on 2580 and 2684 Ma in a probability distribution plots (Collins *et al.*, 2004), although some age peaks are unknown on the Tanzanian Craton. In addition, zircons from sample T06-27 yield a large peak at 2007 ± 4 Ma, which is interpreted as the age of metamorphism (Brick, unpublished data). This is

similar to the findings from Möller *et al*. (1995) and Collins *et al*. (2004). Hence, it can be concluded that the sediments were deposited before the orogeny.

5.2 Sm-Nd isotopic composition

All the Sm-Nd isotopic results are listed in table 2. Furthermore, additional samples from Möller *et al.* (1998), including one eclogite, three pelite and three (one repeated) samples from the Tanzanian Craton are listed in Table 3.

The five eclogitic samples yielded $\varepsilon Nd_{(0)}$ values which range between -17.0 – 1.3. Eclogite facies metamorphism occurred at about 2.0 Ga (Möller *et al.*, 1995; Collins *et al.*, 2004). Therefore, the $\varepsilon Nd_{(2\ Ga)}$ values range from -3.0 to 2.4 at 2 Ga (Figure 8a). An errorchron age for the eclogites of 2281 ± 580 Ma is calculated based on the Sm-Nd data (initial $^{143}Nd/^{144}Nd$ of 0.50969±0.00071, MSWD = 50) (Figure 8b). The $^{147}Sm/^{144}Nd$ ratios of the samples lie within the range of 0.1374 – 0.2316. Although the error is big, it generally indicates that protoliths of the eclogitic rocks are formed before metamorphism at 2.0 Ga.

The results of the five eclogites show average of positive and negative $\varepsilon Nd_{(2\ Ga)}$ values which imply that they are not likely derived from a depleted source. In other words, these samples do not show MORB-like characteristics in their Nd isotopic compositions. However, these irregular isotopic patterns may be due to the presence of contaminations in the protolith. Source of contaminations may be sediments from cratons or volcanic arc within the oceanic plate.

The three mafic samples, on the other hand, give uniform $\varepsilon Nd_{(0)}$ values ranging from -19.0 to -20. The $\varepsilon Nd_{(2\ Ga)}$ values are between -4.0 to -3.0, clearly indicating they are not solely derived from depleted mantle and probably contamination is involved. This is consistent with the geochemical results mentioned in previous section that they formed in subduction-related arc setting.

Similar to the mafic rock samples, the $\varepsilon Nd_{(2\ Ga)}$ values of two pelitic samples are -3.7 and -9.0.

Results are plotted in the Nd evolution diagram (Figure 8a). The Nd evolution diagram shows that all eclogitic and pelitic samples, including those from Möller *et al.* (1998), plot between the evolution path of the depleted mantle and the Tanzanian Craton. This provides support that the contamination of eclogite and mafic rocks are probably derived from the craton.

5.3 Summary

Based on the differences between the major and trace elements compositions as well as the REE patterns, the eclogitic and the mafic rocks are formed from different protoliths. The eclogitic rocks are classified as primitive tholeiitic basalt with some MORB affinity while the mafic rocks are probably cumulates and is subduction-related andesitic basalt. The same conclusion is drawn from the Harker diagrams (Figure 7) where the major oxides (except MgO) and some trace elements are plotted against Mg#. The mafic samples show linear trends in most of the major oxides and trace elements, indicating that they are derived from a single parental source. The eclogitic samples also show a linear relationship though the trends are relatively scattered. However, the negative correlation of Ti with Mg# suggests that the variations are caused by the same process and the scattering is probably caused by weathering and metamorphism after the protolith formation (Stosch and Lugmair, 1990). Furthermore, although the eclogitic and mafic samples are derived from different sources, according to their relative locations in the field, they probably associated with the same subduction tectonic setting but represent different part in the setting.

The high Cr, Ni and the HREE abundance in the pelites suggest that there are some mafic inputs to their protolith. This source may be Archaean greenstones from the Tanzanian Craton, although greenstones are not currently exposed in the southern part of the craton. But the initial εNd values of the pelites plot between the depleted mantle and the Tanzanian Craton εNd evolution paths (figure 8a). This indicates that the sources for the protolith of pelites cannot be derived solely from felsic Tanzanian Craton.

The major element contents, normalized trace elements and REE patterns indicate the protoliths of the Usagaran eclogitic rocks are very likely to be E-MORB, although the large ion lithophile elements (LILE) and the irregular excess in LREE, the Sm-Nd

isotopic compositions in the samples are not consistent with this conclusion. In general, chondrite normalized REE plots of N-MORB show a slight LREE depletion comparing to heavy rare earth element (HREE) while the LREE are only slightly enriched when compared with HREE for E-MORB (Figure 4c).

There are a number of possible reasons for these inconsistencies: 1) the eclogites may actually represent another type of basalt, such as island-arc basalt, instead of MORB; 2) the eclogites formed from subducting MORB but with some contaminations during the process; 3) the mechanism of plate tectonics 2 billion years ago is fundamentally different from the modern plate tectonics and hence the geochemical compositions of MORB are different from the modern Earth. For the first possibility to apply the rock type classifications based on the discrimination diagrams and trace elements would need to be incorrect, which would require significant mobility of those elements applied. An investigation on the mobility of the trace elements and REE would give some ideas on this possibility. The second possibility involves additional materials input to the MORB before or during subduction: the geochemical compositions of the associated (sedimentary) rocks may provide some clues about this assumption. The last possibility concerns the thermal and geochemical evolution of the Earth. Comparison of eclogitic rocks in this study to other eclogites or even oceanic crust fragments in different ages will perhaps give some hints about this suggestion. All possibilities will be discussed in the later sections.

The spidergram and REE patterns of the mafic rocks show that they are not MORB. Strong depletions in Nb clearly indicate that these rocks are subduction-related. In addition, they are classified as continental tholeiites in the TiO_2-K_2O-P_2O_5 discrimination diagram. Therefore, the mafic rocks are probably formed in a subduction-related continental arc setting.

6. Discussion

6.1 Geochemical characteristics of MORB and factors influencing them

As mentioned in the introduction, MORB is tholeiitic basalt that formed from mantle beneath the oceanic ridge by decompression melting. Identification of MORB from other

types of basalt is based on its unique trace element fingerprint. In general, MORB tends to show LILE and LREE depleted patterns in chondrite- or primitive mantle-normalized spidergrams. The maximum concentrations of the moderately incompatible elements in MORB are about 10 times of the primitive mantle values (Hofmann, 1988).

MORB can be divided into two categories based on their differences in LILE and LREE concentrations: normal-type MORB (N-MORB) and enriched-type MORB (E-MORB). N-MORB is characterized by low highly incompatible elements content, while E-MORB is enriched in highly incompatible elements (Sun *et al.*, 1979). They can be distinguished from each other by their normalized REE patterns. N-MORB shows LREE depletion in chondrite-normalized REE plots. E-MORB, on the other hand, has a LREE enriched pattern in the chondrite-normalized REE plot. Apart from the REE patterns, N-MORB and E-MORB can also be distinguished by their normalized spidergram pattern. The eclogitic samples show enriched LREE and a flat HREE pattern in chondrite-normalized plot and hence, they are derived from E-MORB. However, the magnitudes of the enrichments are higher than a typical E-MORB. Therefore, it is worthwhile to consider factors affecting the generation of MORB along the oceanic ridge.

Sun and McDonough (1989) pointed out that there are four factors influencing chemical and isotopic characteristics of basaltic magma: 1) the source characteristics, which are a function of its previous history; 2) the tectonic environment of magma generation; 3) magma generation conditions and processes; and 4) mixing of different mantle source regions. MORB generate along the oceanic ridges where there is generally no other type of crust around. Therefore, the effect of the second and fourth factors on the chemical and isotopic characteristics should be minimal and can be excluded from considerations.

The first factor considers the geochemical variations in the mantle. Seismological evidence shows that the Earth's mantle is separated into two layers at about 660 km and this is probably due to mineralogical and/or chemical differences. The upper and lower layers may interact and cause chemical variations in the mantle. For example, the subducted slabs can penetrate into the lower mantle while plumes from the lower mantle may rise and pass through the upper mantle to the surface (Olson *et al.*, 1990; Machetel

and Weber, 1991; Stein and Hofmann, 1994). In addition, recycling of oceanic crust and lithosphere may also be important to generating mantle heterogeneities (Hofmann, 1997).

The third factor that Sun and McDonough (1989) described as influencing the chemical composition of basaltic magma focuses on how MORB is generated. As mentioned before, MORB is formed from mantle beneath the oceanic ridge by decompression melting. Factors such as spreading rate of the ridge, temperature of the mantle, presence of water etc., will affect the degree of melting which in turn affect the chemical compositions of melt. Water will lower the melting temperature of the mantle and hence, more melt will be generated at the same temperature in the presence of water. More melt will also be generated if the temperature of the mantle that approaching the surface is higher than normal. Once partial melting occurs, the highly incompatible elements such as LILE, will rapidly go into the melt first until they are exhausted. As the magnitude of partial melting increases, concentrations of the highly incompatible elements decrease. On the other hand, the degree of partial melting is related to the spreading rate of the ridge: the higher the spreading rate of the ridge, the lower the pressure along the ridge, resulting in a higher degree of partial melting. Therefore, larger volumes of relatively depleted melt will be generated.

The E-MORB affinity of the Usagaran eclogitic rocks are probably due to an enriched source and/or a low degree of mantle melting, although it is difficult to quantify the influence of these two factors. However, since the protoliths of the eclogitic rocks are formed in the Palaeoproterozoic, other factors such as the thermal regime of the Earth at that time may also affect MORB generation and this will be discussed in later section.

6.2 Mobility of elements during metamorphism

Apart from rock classifications, major and trace elements are often used together in identifying the original tectonic settings of igneous rocks (Rollinson, 1995). They are also applied to distinguish the tectonic settings in which metamorphosed igneous rocks like eclogite originally formed (e.g. Liu *et al.*, 2005; Song *et al.*, 2006; Kullerud *et al.*, 1990). Validity of these interpretations depends not only on the original element content of protoliths but also on the sensitivity of these elements to alteration. Therefore, it is essential to know the behavior of these elements during metamorphism and weathering.

Geochemical compositions of rocks can be altered under many circumstances. There are two possible circumstances for the eclogitic rocks in this study to undergo massive alteration. The first one is caused by interactions with seawater and/or hydrothermal fluid. The second one occurs during subduction as the rocks are subjected to high-pressure low-temperature metamorphic conditions, where they react with the fluids generated by dehydration as well as the surrounding mantle.

It is commonly thought that altered submarine basalts are enriched in incompatible elements, such as LILE and B. Studies point out the altered submarine basalts are enriched in K, Rb, Cs, Li and B (Hart *et al.*, 1974; Sayfried *et al.*, 1998) while enrichment or depletion of Ba can be up to about 50% (Philpotts *et al.*, 1969). In addition, there are geochemical data from high-pressure and ultrahigh-pressure metabasaltic and metasedimentary rocks that demonstrate at least local-scale of LILE mobility when their protoliths subducted to great depths, although they generally represent relatively small fraction of loss distributed over large volumes of rocks (Bebout, 2007). This may lead to a significant flux of LILE to the mantle, but in many cases there is no obvious depletion signature left in the sources (Spandler *et al.*, 2004; Bebout, 2007).

From the normalized spidergrams (Figure 4a & 4b), the eclogitic samples are enriched in Ba and U, and depleted in Rb, Sr and K (except sample T01-40, which shows enrichment in K). These LILE variations are probably caused by seafloor alteration of the protolith. On the other hand, as mentioned previously, the eclogitic and mafic rocks may come from the same subduction tectonic setting. LILE enrichments of the mafic rocks could be due to the fluid generated by slab dehydration during subduction as LILE are liberated from the slab to the fluid phase. Although the LILE are highly mobile during weathering and metamorphism, they do not affect the interpretations in this study as they are not used to indentify protoliths.

The REE are considered to be relatively stable under seawater and hydrothermal fluid alterations as well as metamorphism. Experimental (e.g. Hajash, 1984) and petrologic studies (e.g. Philpotts *et al.*, 1969; Tribuzio *et al.*, 1996) imply that the abundances and distribution patterns of REE are basically identical as there are no significant differences before and after alteration. Hajash (1984) claimed that although

some leaching or redistribution of REE, especially the LREE, may occur during hydrothermal alteration, the whole-rock REE patterns may still be used as petrogenetic indicators.

The high field strength elements (HFSE) are normally considered as immobile elements in most geological processes. They are used as indicators to discriminate among different sources of magma from different geological settings (e.g. Pearce and Cann, 1973; Shervais, 1982; Meschede, 1986). However, there is evidence indicating that they can be transported by a variety of solutions in magmatic, metamorphic and hydrothermal environments under certain conditions, although their mobility depends on many factors such as P-T conditions, pH of the solutions and fluid chemistry (Jiang *et al.*, 2005). Therefore, abundances of HFSE can be altered under appropriate conditions.

In general, the HFSE and REE abundances of the eclogitic rocks are not significantly altered by weathering and metamorphism. Sample T07-16, which was penetrated by vein quartz, shows similar pattern in the spidergrams although there are strong depletions in Nb, Sr and weak depletion in Ti. In addition, the concentrations of REE are generally lower than other eclogitic samples but in a same magnitude throughout the series. These fit the conclusions made by the previous workers that the HFSE and REE are generally not affected by weathering and metamorphism. This also applied to the HFSE and REE abundances of the mafic rocks.

Based on the geochemical data of the eclogitic as well as mafic samples and the mobility of elements in weathering and metamorphism, two conclusions can be drawn. First, variations in LILE and other incompatible elements in the eclogitic and mafic rocks are caused by seafloor alteration and dehydration of subducting slabs respectively. Second, the HFSE and REE compositions remain undisturbed through time and hence, they are suitable to be used in the discrimination diagrams to identify their sources. However, the LREE enrichments on both rock types are not consistent with this finding. There must be some other factors affecting the LREE enrichments in these rocks and this issue will be discussed in a later section.

Pearce and Cann (1973) pointed out that for an element or combination of elements to be useful in characterizing the different magma types, they must have a greater variation in concentration among different magma types than between samples of the same magma type and be insensitive to secondary processes such as weathering and metamorphism. Some elements, for example, Ba, vary significantly between ocean-floor and volcanic arc basalts (Pearce and Cann, 1973) but are very mobile during weathering and metamorphism (Philpotts *et al.*, 1969) and hence not suitable to be used in distinguishing different magma types.

Kullerud *et al.* (1990) investigate the mobility of elements in their samples by plotting the elements of interest against Zr. A good correlation between Zr and an element indicated the mobility of the element during post-magmatic processes could be considered as negligible (Kullerud *et al.*, 1990). This method is applied here in order to test the mobility of Ti, Sr, Y, V, and Nb in the eclogitic and mafic samples as they are used in the discrimination diagrams (Figure 7). Results show that all elements except Sr have a fairly strong correlation with Zr, which suggests they are not very mobile during post-magmatic alteration or metamorphism. In contrast, the Sr against Zr plot shows a scattered pattern which means that Sr concentrations were altered after rock formation. Although the magnitude of the mobility of Sr may be small, discrimination diagrams that involved Sr are not suitable to be used as evidence to support or refute the argument that the eclogitic rocks formed from MORB.

6.3 Feasibility of identifying Proterozoic plate tectonics based on modern plate tectonic characteristics

Geochemical compositions of rocks offer some constraints on rock evolution (Sun *et al.*, 1979). Information such as sources of rocks, tectonic environments and metamorphic processes can be revealed if the geochemical data are interpreted appropriately. This study has used the major element and trace element compositions as well as Sm-Nd isotopic data to investigate whether the rocks from Usagaran Belt had experienced subduction. However, as those interpretations are based on knowledge from relatively young plate tectonics settings, it is necessary to examine if this knowledge is applicable

to Proterozoic situations. In other words, it is necessary to investigate if the tectonic settings in the Proterozoic are the same as what is now seen.

There are a number of workers using discrimination diagrams from different authors to identify the source of their samples, including samples from Precambrian (e.g. Coish and Sinton, 1991; Dann, 1991; Dostal and McCutcheon, 1990; Khan *et al.*, 2005). Discrimination diagrams, including those were not used in this study, are not widely applied because they do not always function properly (Rollinson, 1995). To demonstrate this, two well-described Proterozoic ophiolite complexes are chosen to test whether the discrimination diagrams that have been applied in this study are able to identify MORB from other types of basalts. Ophiolite complexes are sequences of rock types consisting deep-sea sediments lying above basaltic pillow lavas, dykes, gabbro and ultramafic peridotite. Some of them are the remnants of oceanic crust while some formed in back-arc basins. They are brought to the surface by obduction, a lateral, sub-horizontal displacement of a lithospheric plate onto a continental margin. They are chosen because they are oceanic crustal rocks, the same as the assumed protolith of Usagaran eclogitic rocks. In addition, samples with similar ages as the eclogitic rocks are selected to see if these diagrams are able to identify ancient basaltic rocks, at least to 2 Ga.

The two chosen ophiolite complexes are the 1.95 Ga Jormua Ophiolite from northeastern Finland (Peltonen *et al.*, 1996) and the 1.9 Ga Flin Flon Belt from Canada (Stern *et al.*, 1995). The Jormua Ophiolite complex is composed of two types of basalts which differ in geochemical compositions (Peltonen *et al.*, 1996). The 'early dykes' have OIB-like trace element patterns while the remaining dykes and all lavas show E-MORB affinity (Peltonen *et al.*, 1996). Three types of basalts are found in the Flin Flon Belt based on their geochemical signatures: the N-MORB and E-MORB ocean-floor basalts as well as some OIB-liked basalt (Stern *et al.*, 1995). Data from Peltonen *et al.* (1996) and Stern *et al.* (1995) are plotted on the discrimination diagrams (Figure 10).

The Jormua basalts with E-MORB affinity generally fall into the MORB field. However, the samples spread in the island-arc tholeiite field and the MORB field in the Ti-Zr-Sr discrimination diagram. This is probably due to the mobility of Sr through time and this problem has been mentioned by Pearce and Cann (1973). They are plotted in the

MORB field in the Ti-Zr discrimination diagram which is for altered samples (Pearce and Cann, 1973). The samples are scattered along the boundary of N-MORB and E-MORB in the Nb-Zr-Y diagram proposed by Meschede (1986) and some of them plotted out of the MORB field.

Similar problems occur with classification of the basalt from Flin Flon Belt. However, one interesting thing to note is although the samples are mis-classified in the Ti-V discrimination diagram, it looks like these mis-classifications are systematic, i.e., samples with OIB affinity are plotted into the MORB field and samples with MORB affinity are classified as arc tholeiite. This may caused by the relative low concentrations in Ti in these samples (Stern *et al.*, 1995).

In general, the discrimination diagrams are mostly able to classify Proterozoic samples into the right category, but mis-classifications do occur, indicating that the discrimination diagrams do not always function properly. There are many factors, such as the initial concentration of the source and post-depositional processes, affecting the trace element concentrations of rocks. Therefore, geochemical compositions of rocks may vary if they are from similar settings or even in the same suite. Although different tectonic environments do have distinctive geochemical signatures which can be used as indicators for identification, care should be taken when handling the data and they should not be used as a critical evidence for classification (Rollinson, 1995).

The normalized trace element pattern of a sample, on the other hand, is widely used to distinguish different tectonic settings. It is controlled by the chemical compositions of the source and the crystal-melt equilibria which have taken place during its evolution path (Rollinson, 1995).

It is generally accepted that the Earth was hotter in the past. There were more radioactive isotopes present in the mantle. Mantle convection was probably more vigorous and the lower mantle possibly was involved as well (Sun and McDonough, 1989). In addition, hotter mantle may cause larger scale mantle melting. These factors would affect the geochemical composition of the melt. Since the geochemical compositions of MORB are strongly related to their mantle source and the degree of

decompressional melting, it is not surprising that the geochemical compositions of ancient MORB are different from the modern ones. Sun and Nesbitt (1977) listed some ratios of lithophile elements in Archaean basalt and modern MORB and claimed that they can be treated as good indicators of geochemical contents of mantle through time as they are almost independent from the degree of partial melting. The ratios showed that the Archaean basalts are more enriched in LILE and LREE compared with modern MORB while the abundances of less incompatible elements such as the HFSE are similar though time (Sun and Nesbitt, 1977). That means the Archaean mantle is enriched in LILE and LREE and hence, it is reasonable to assume that the Archaean MORB is also enriched in those elements because of its enriched source.

As the geochemical fingerprints of MORB are based on the concentrations of HFSE and HREE which do not change dramatically through time, they are suitable to be used in identifying the protoliths of most rocks from different ages, including the Palaeoproterozoic Usagaran eclogitic rocks. In fact, normalized spidergrams and REE plots are very commonly presented in published work as part of the geochemical evidence to prove rocks are derived from certain protoliths. Examples include the early Archaean Isua Supracrustal Belt (Komiya *et al.*, 2004), the early Proterozoic komatiitic basalts from the Vetreny Belt in the southeastern Baltic Shield (Puchtel *et al.*, 1997) and the Ordovician eclogitic rocks from Ligurian Alps (Giacomini *et al.*, 2007).

To conclude, the discrimination diagrams that have been used in this study are suitable to indentify rock sources at least from the Palaeoproterozoic although care has to be taken. However, the normalized diagrams are powerful tools that have been used to identify rocks from different ages, and results based on them should be reliable. Hence, the interpretations of the protoliths of the rock samples in this study are very likely to be reliable as well.

6.4 Sm-Nd isotopic composition and its significance

Apart from age determination, Sm-Nd isotopic compositions can be also applied to identify the origin of the rocks. The main advantage of Sm-Nd radioactive pair is they are both REEs which are relatively insensitive to metamorphism or alteration after rock formation and hence, the system is less likely to be disturbed (DePaolo, 1988). This has

also been discussed in the previous section. In addition, the mass differences among the Nd isotopes are very small, so they cannot be fractionated by magmatic processes (Rollinson, 1995) and the same situation happens to Sm. Therefore, any changes to the resulting isotopic ratios can only be caused by the radioactive decay and/or contamination during petrogenesis.

For determining ages, the decay path that is of interested is the radioactive isotope ^{147}Sm decays by alpha emission to a stable isotope ^{143}Nd with a long half life (106 billion years) by the following equation (Bowen, 1988; DePaolo, 1988):

$$^{147}_{62}\mathrm{Sm} \rightarrow ^{143}_{60}\mathrm{Nd} + ^{4}_{2}\mathrm{He}$$

Assuming the increased ^{143}Nd/^{144}Nd is caused by the decay of ^{147}Sm only, the measured ^{143}Nd/^{144}Nd in a rock at present is equal to its initial ^{143}Nd/^{144}Nd plus the amount of decayed ^{147}Sm, which can be calculated from the measured ^{147}Sm/^{144}Nd at present. Therefore, the initial ^{143}Nd/^{144}Nd can be calculated by the following equation:

$$\left[\frac{^{143}\mathrm{Nd}}{^{144}\mathrm{Nd}}\right]_{t(0)} = \left[\frac{^{143}\mathrm{Nd}}{^{144}\mathrm{Nd}}\right]_{t(initial)} + \left[\frac{^{147}\mathrm{Sm}}{^{144}\mathrm{Nd}}\right]_{t(0)} \left(e^{\lambda t} - 1\right),$$

where $\left[\frac{^{143}\mathrm{Nd}}{^{144}\mathrm{Nd}}\right]_{t(0)}$ and $\left[\frac{^{147}\mathrm{Sm}}{^{144}\mathrm{Nd}}\right]_{t(0)}$ are the measured Nd isotopic ratio and Sm-Nd radioactive isotopic pair ratio in the rock at present respectively, $\left[\frac{^{143}\mathrm{Nd}}{^{144}\mathrm{Nd}}\right]_{t(initial)}$ is the Nd isotopic ratio at the time when the rocks formed, t is the time and λ is the decay constant which is 6.54 x 10^{-12} for ^{147}Sm.

Although both Sm and Nd are REE, they differ in compatibility due to the slight differences in their atomic radii. Sm tends to enter the crystal lattice easily while Nd tends to stay in the melt during crystallization or melting. Hence, the Sm/Nd ratio in mafic rocks will be higher than in felsic rocks. This differentiation will eventually lead to higher ^{143}Nd/^{144}Nd in mafic rocks than in felsic rocks. Thus the protolith of rocks can be determined by this isotopic ratio fingerprint. As with the REE patterns, Nd isotope ratios

are only comparable if they are 'normalized' to an expected value from a uniform reservoir trend (Rollinson, 1995). The εNd in this study represents the Nd isotope ratios of the samples normalized to the Nd isotope ratio of depleted mantle with time:

$$\varepsilon Nd_t = \left[\frac{{}^{143}Nd/{}^{144}Nd_{sample,t}}{{}^{143}Nd/{}^{144}Nd_{DM,t}} - 1 \right] \times 10^4 ,$$

where ${}^{143}Nd/{}^{144}Nd_{sample,t}$ represents the ratio of a rock in particular time t, and ${}^{143}Nd/{}^{144}Nd_{DM,t}$ stand for the ratio of the depleted mantle at the same time.

Trace elements and REE compositions show that the protolith of the Usagaran eclogitic rocks is E-MORB which is derived from the mantle and hence, their εNd should be positive. However, results show that the $\varepsilon Nd_{2\ Ga}$ values from five eclogitic samples range from -4.0 to 2.4, which are more negative than expected. Two possible explanations account for these results. The εNd variations may be caused by the magmatic evolution path of the protolith, if the protolith of those eclogitic rocks is derived from a slightly enriched depleted mantle (Paquette *et al.*, 1989). The second possibility is contamination of protolith by sediments or even continental crust during subduction.

If the first possibility is the case, all samples should have similar evolution paths through time. That means the εNd evolution paths of all samples should have either positive or negative slopes. However, the εNd evolution paths of the eclogitic samples give out both positive and negative slopes. This clearly indicates that the variances in εNd are not caused by the magmatic evolution path of the protolith.

Contamination by sediments or continental crust can result in a range of εNd values reflecting the degree of contamination, thus the slope of εNd evolution path of the samples can be both positive and negative. The effect of this kind of contamination can be localized, which means the variation in εNd can be very large within a small area. Furthermore, small amount of sediments derived from craton or crustal materials can result in very large contamination as the absolute amounts of Sm and Nd in continental crusts are very high, though their Sm/Nd ratio can be low.

The mafic rocks in this study all gave negative $\varepsilon Nd_{2\ Ga}$, indicating they have a continental affinity. This is consistent with the conclusion, based on the trace elements compositions and chondrite-normalized REE patterns, that the mafic rocks were once part of the sub-continental mantle.

6.5 Comparisons with other eclogites from similar settings

Table 4 summarizes a brief comparison among eclogites from the Usagaran Orogenic Belt, Dulan Belt of China and the Alpine External Crystalline Massifs (AECM). All eclogites occur as lenses or layers in highly metamorphosed rock strata. Most of the protoliths of the eclogitic samples are either N-MORB or E-MORB with some crustal contamination according to their REE patterns and/or initial εNd values. However, these eclogites have different peak metamorphic conditions. Of these, the Usagaran Orogenic Belt has the highest peak temperature up to 800ºC (Brick, unpublished data), while the peak pressure is about 18 kbar (Möller *et al.*, 1995; Brick, unpublished data). Compared with the Dulan Belt in China, although the peak pressure is up to 33 kbar, the peak temperature is about 780ºC (Song *et al.*, 2003). In other words, although the Cambrian Dulan Belt eclogites formed deep in the mantle, their peak temperatures are not as high as the Palaeoproterozoic Usagaran Belt eclogites. This leads to a conclusion that the Palaeoproterozoic Earth is warmer that the Cambrian Earth.

There are a number of line of evidence that reflect that the early Earth is warmer than the modern Earth (e.g. Turcotte; 1980; Richter, 1985; Grove and Parman, 2004; Brown, 2007). Where subduction of oceanic crusts occurred in the early history of the Earth, it may have been too warm to preserve eclogitic mineral assemblages. This may explain the rare occurrence of eclogite in the early Earth history. Provided the Earth is warmer in its early history, it can be assumed that the subduction products are not eclogite but some higher temperature metamorphic mineral assemblage, such as granulite facies. In fact, the peak metamorphism of eclogite from Usagaran Belt reached to the granulite facies (Brown, 2007; Collins *et al.*, 2004). On the other hand, the slabs may also not have been deeply subducted enough as warmer crust is less dense so subduction would be shallower and hence, low-pressure high-temperature mineral assemblages may also be the mark of ancient subduction zones.

6.6 Possible tectonic setting

Based on the geochemical data and the field relation among the eclogites, mafic rocks and pelites, a possible tectonic setting is suggested. The protolith of the eclogites, i.e., the E-MORB, formed along a mid-ocean ridge at about 2.2 Ga (Möller *et al.* 1995). Various sediments from different sources, including the Tanzanian Craton, are deposited on it as seafloor sediments. The E-MORB was subducted beneath the Tanzanian Craton at 2 Ga (Möller *et al.*, 1995; Collins *et al.*, 2004). The subducted E-MORB came back to the near surface due to exhumation which probably caused by detachment of subducting slab and slab roll back. The mafic rocks, which derived from the mantle, were attached to the exhuming slab returned to the surface. This also led to the formation of a basin for deposition of the Konse Group.

7. Conclusion

The protolith of the eclogitic rocks from Usagaran Orogenic Belt are verified by analyzing the bulk-rock chemistry and Sm-Nd isotopic composition. A few conclusions can be drawn from this study:

- The geochemical figures of the eclogitic rocks from Usagaran Orogenic Belt are similar to present-day E-MORB with LILE and LREE enrichment. Based on the variations in initial εNd values and their differences in evolution paths, there are probably some contamination caused by crustal materials derived from the Tanzanian Craton.
- The mafic rocks are derived from the mantle. Strong Nb depletions indicate that they are subduction related. Enrichments in LILE and LREE are probably caused by the dehydration of subducting slab plus some crustal derived materials.
- The protolith of the pelite is shale, and the sediments are mainly derived from the Tanzanian Craton with a significant mafic input according to their geochemical characteristics and εNd values.
- According to their field relations as well as geochemical compositions, the eclogites, mafic rocks and pelites come from the same subduction setting that operated *ca.* 2 Ga.
- Despite the fact that the Earth was hotter in its early history, modern plate tectonics, (i. e., subduction of cold oceanic crust into a warm mantle resulting in high-pressure

low-temperature metamorphism), occurred and was recorded in the Usagaran Belt during the Palaeoproterozoic. Thus modern-style plate tectonics have operated since at least 2.0 Ga.

8. Acknowledgements

This work was funded by Australian Research Council Discovery grant DP0774019 to A. S. Collins. I thank to my supervisor, Karin Barovich and Alan Collins, for their guidance and help throughout the academic year. Thanks also go to John Stanley and David Bruce for their help in sample preparations as well as sample analysis. Rachael Brick are thanked for her kindly help on completing the project, especially her assistance and comments on this thesis. Thanks must give to the honours students of 2009, in particular Jade Palmer and Denise Yong. Tessa Lane and Andrew Fernie are thanked for their comment on the draft. Last but definitely not least, I thank my family for their support, even though I am geographically apart from them for my dream.

9. References

AOYA M., TSUBOI M. & WALLIS S. R. 2005. Origin of eclogitic metagabbro mass in the Sambagawa belt: Geological and geochemical constraints. *Lithos* **89**, 107-134.

ARCULUS R. J. 1987. The significance of source versus process in the tectonic controls of magma genesis. *Journal of Volcanology and Geothermal Research* **32**, 1-12.

BALDWIN J. A., BOWRING S. A., WILLIAMS M. L. & WILLIAMS I. S. 2004. Eclogites of the Snowbird tectonic zone: petrological and U-Pb geochronological evidence for Paleoproterozoic high-pressure metamorphism in the western Canadian Shield. *Contrib Mineral Petrol* **147**, 528-548.

BEBOUT G. E. 2007. Metamorphic chemical geodynamics of subduction zone. *Earth and Planetary Science Letters* **260**, 373-393.

BECKER H., JOCHUM K. P. & CARLSON R. W. 2000. Trace element fractionaton druing dehydration of eclogites from high-pressure terranes and the implications for element fluxes in subduction zones. *Chemical Geology* **163**, 65-99.

BLATT H. & TRACY R. J. 1996. *Petrology: igneous, setimentary, and metamophic*. W. H. Freeman and Company, New York.

BOWEN R. 1988. *Isotopes in the Earth Sciences*. Elsevier Applied Science Publishers Ltd, Essex.

BROWN M. 2007. Metamorphic Conditons in Orogenic Belts: A Record of Secular Change. *International Geology Review* **49**, 193-234.

CANN J. R. 1970. Rb, Sr, Y, Zr and Nb in some ocean-floor basaltic rocks. *Earth and Planetary Science Letters* **10**, 7-11.

COISH R. A. & SINTON C. W. 1992. Ceochemistry of mafic dikes in the Adirondack mountains: implications for late Proterozoic continental rifting. *Contrib Mineral and Petrol* **110**, 500-514.

COLLINS A. S., RADDY S. M., BUCHAN C. & MRUMA A. H. 2004. Temporal constraints on Palaeoproterozoic eclogite formation and exhumation (Usagaran Orogen, Tanzania). *Earth and Planetary Science Letters* **224**, 175-192.

DANN J. C. 1991. Early Proterozoic ophiolite, central Arizona. *Geology* **19**, 590-593.

DEPAOLO D. J. 1988. *Neodymium Isotope Geochemistry: An Introduction*. Minerals and Rocks. Springer-Verlag, Berlin.

DOSTAL J. & MCCUTCHEON S. R. 1990. Geochemistry of Late Proterozoic basaltic rocks from southeastern New Brunswick, Canada. *Precambrian Research* **47**, 83-98.

FLOYD R. A. & WINCHESTER J. A. 1978. Identification and discrimination of altered and metamorphosed volcanic rocks using immobile element. *Chemical Geology* **21**, 291-306.

GIACOMINI F., BRAGA R., TIEPOLO M. & TRIBUZIO R. 2007. New constraints on the origin and age of Variscan eclogitic rocks (Ligurian Alps, Italy). *Contrib Mineral Petrol* **153**, 29-53.

GOLDSTEIN S. L., O'NIONS R. K. & HAMILTON P. J. 1984. A Sm-Nd isotopic study of atmospheric dust and particulates from major river systems. *Earth and Planetary Science Letters* **70**, 221-236.

GROVE T. L. & PARMAN S. W. 2004. Thermal evolution of the Earth as recorded by komatiites. *Earth and Planetary Science Letters* **219**, 173-187.

HAJASH JR. A. 1984. Rare earth element abundace and distribution patterns in hydrothermally altered Basalts: experimental results. *Contrib Mineral Petrol* **85**, 409-412.

HART S. R. 1969. K, Rb, Cs contents and K/Rb, K/Cs ratios of fresh and altered submarine basalts. *Earth and Planetary Science Letters* **6**, 295-303.

HART S. R., ERLANK A. J. & KABLE E. J. D. 1974. Sea Floor Basalt Alteration: Some Chemical and Sr Isotopic Effects. *Contrib Mineral and Petrol* **44**, 219-230.

HERMS P. 2002. Fluids in a 2 Ga old subduction zone-deduced from eclogite-facies rocks of the Usagaran belt, Tanzania. *European Journal of Mineralogy* **14**, 361-373.

HOFMANN A. W. 1988. Chemical differentiation of the Earth: the relationship between mantle, continental crust, and oceanic crust. *Earth and Planetary Science Letters* **98**, 297-314.

HOFMANN A. W. 1997. Mantle geochemistry: the message from oceanic volcanism. *Nature* **385**, 219-299.

JAHN B.-M., CABY R. & MONIE P. 2001. The oldest UHP eclogites of the World: age of UHP metamorphism, nature of protoliths and tectonic implications. *Chemical Geology* **178**, 143-158.

JIANG S.-Y., WANG R.-C., XU X.-S. & ZHAO K.-D. 2005. Mobility of high field strength elements (HFSE) in magmatic-, metamorphic-, and submarine-hydrothermal systems. *Physics and Chemistry of the Earth* **30**, 1020-1029.

KHAN M. S., SMITH T. E., RAZA M. & HUANG J. 2005. Geology, Geochemistry and Tectonic Significance of Mafic-ultramafic Rocks of Mesoproterozoic Phulad Ophiolite Suite of South Delhi Fold Belt, NW Indian Shield. *Gondwana Research* **8**, 553-566.

KOMIYA T., MARUYAMA S., HIRATA T., YURIMOTO H. & NOHDA S. 2004. Geochemistry of the oldest MORB and OIB in the Isua Supracrustal Belt, southern West Greenland: Implications for the compositon and temperature of early Archean upper mantle. *The Island Arc* **13**, 47-72.

KULLERUD K., STEPHENS M. B. & ZACHRISSON E. 1990. Pillow lavas as protoliths for eclogites: evidence from a late Precambrian-Cambrian continental margin, Seve Nappes, Scandinavian Caledonides. *Contrib Mineral and Petrol* **105**, 1-10.

LI Z., YANG J., XU Z., LI T., XU X., REN Y. & ROBINSON R. T. 2009. Geochemistry and Sm-Nd and Rb-Sr isotopic composition of eclogite in the Lhasa terrane, Tibet, and its geological significance. *Lithos* **109**, 240-247.

LIU Y., LI S., XU S., JAHN B.-M., ZHENG Y.-F., ZHANG Z., JIANG L., CHEN G. & WU W. 2005. Geochemistry and geochronology of eclogites from the northern Dabie Mauntains, central China. *Journal of Asian Earth Sciences* **25**, 431-443.

LUDDEN J. N. & THOMPSON G. 1979. An evaluation of the behavior of the rare earth elements during the weathering of sea-floor basalt. *Earth and Planetary Science Letters* **43**, 85-92.

MACHETEL P. & WEBER P. 1991. Intermittent layered convection in a model mantle with an endothermic phase change at 670 km. *Nature* **350**, 55-57.

MESCHEDE M. 1986. A method of discriminating between different types of mid-ocean ridge basalts and continental tholeiites with the Nb-Zr-Y diagram. *Chemical Geology* **56**, 207-218.

MILLER C. & THONI M. 1997. Eo-Alpine eclogistsation of Permian MORB-type gabbros in Koralpe (Eastern Alps, Austria): new geochronological, geochemical and petrological data. *Chemical Geology* **137**, 283-310.

MOLLER A., APPEL P., MAEZGER K. & SCHENK V. 1995. Evidence for a 2 Ga subduction zone: Eclogites in the Usagaran belt of Tanzania. *Geological Society of America* **23**, 1067-1070.

MOLLER A., MEZGER K. & SCHENK V. 1998. Crustal Age Domains and the Evoluton of the Continental Crust in the Mozabique Belt of Tanzania: combined Sm-Nd, Rb-Sr, and Pb-Pb Isotopic Evidence. *Journal of Petrology* **39**, 749-783.

MOORES E. M. 2002. Pre-1Ga (pre-Rodinian) ophiolites: Theri tectonic and environmental implications. *Geological Society of America Bulletin* **114**, 80-95.

MRUMA A. H. 1989. Stratigraphy, Metamorphism and Tectonic Evolution of the Early Proterozoic Usagaran Belt, Tanzania. University of Oulu, Finland (unpubl.).

MUNKER C., WORNER G., YOGODZINSKI G. & CHURIKOVA T. 2004. Behaviour of high field strength elements in subduction zones: constraints from Kamchatka-Aleutian arc lavas. *Earth and Planetary Science Letters* **224**, 275-293.

MURMA A. H. 1995. Stratigraphy and palaeodepositional environment of the Palaeoproterozoic volcano-sedimentary Konse Group in Tanzania. *Journal of African Earth Sciences* **21**, 281-290.

OLSON P., SILVER P. G. & CARLSON R. W. 1990. The large-scale structure of convection in the Earth's Mantle. *Nature* **344**, 209-215.

PAQUETTE J. L., MENOT R. P. & PEUCAT J. J. 1989. REE, Sm-Nd and U-Pb zircon study of eclogites from the Alpine Ecternal Massifs (Western Alps): evidence for crustal contamination. *Earth and Planetary Science Letters* **96**, 181-198.

PEARCE J. A. 2008. Geochemical fingerprinting of oceanic basalts with application to ophiolite classification and the search for Archean oceanic crust. *Lithos* **100**, 14-48.

PEARCE J. A. & CANN J. R. 1971. Ophiolite origin investigated by discriminant analysis using Ti, Zr and Y. *Earth and Planetary Science Letters* **12**, 339-349.

PEARCE J. A. & CANN J. R. 1973. Tectonic setting of basic volcanic rocks determined using trace element analyses. *Earth and Planetary Science Letters* **19**, 290-300.

PEARCE J. A. & NORRY M. J. 1979. Petrogenetic Implications of Ti, Zr, Y, and Nb Variations in Volcanic Rocks. *Contrib Mineral Petrol* **69**, 33-47.

PEARCE T. H., GORMAN B. E. & BIRKETT T. C. 1975. The TiO_2-K_2O-P_2O_5 Diagram: a method of discrimination between oceanic and non-oceanic basalts. *Earth and Planetary Science Letters* **24**, 419-426.

PELTONEN P., KONTINEN A. & HUHMA H. 1996. Petrology and Geochemistry of Metabasalts from the 1.95 Ga Jormua Ophiolite, Northeastern Finland. *Journal of Petrology* **37**, 1359-1383.

PHILPOTTS J. A., SCHNETZLER C. C. & HART S. R. 1969. Submarine basalts: Some K, Rb, Sr, Ba, rare-earth, H_2O, and CO_2 data bearing on their alteration, modification by plagioclase, and possible source materials. *Earth and Planetary Science Letters* **7**, 293-299.

PUCHTEL I. S., HAASE K. M., HOFMANN A. W., CHAUVEL C., KULIKOV V. S., GARBE-SCHONBERG C.-D. & NEMCHIN A. A. 1997. Petrology and geochemistry of crustally comtaminlated komatiitic basalts from the Vetreny Belt, southeastern Baltic Shield: Evidence for an early Proterozoic mantle plume beneath fifted Archean continental lithosphere. *Geochimica et Cosmochimica Acta* **61**, 1205-1222.

RADDY S. M., COLLINS A. S., BUCHAN C. & MRUMA A. H. 2004. Heterogeneous excess argon and Neoproterozoic heating in the Usagaran Orogen, Tanzania, revealed by single grain $^{40}Ar/^{39}Ar$ thermochronology. *Journal of African Earth Sciences* **39**, 165-176.

RADDY S. M., COLLINS A. S. & MRUMA A. 2003. Complex high-strain deformation in the Usagaran Orogen, Tanzania:structural setting of Palaeoproterozoic eclogites. *Tectonophysics* **375**, 101 - 123.

RICHTER F. M. 1985. Models for the Archean thermal regime. *Earth and Planetary Science Letters* **73**, 350-360.

ROLLINSON H. R. 1995. *Using Geochemical Data: Evaluation, Presentation, Interpretation*. Longman Group Limited, Essex, England.

SASSI R., MAZZOLI C., MILLER C. & KONZETT J. 2004. Geohcmistry and metamporphic evolutio of the Pohorje Mountain eclogites from the easternmost Austroalpine basement of the Eastern Alps (Northern Slovenia). *Lithos* **78**, 235-261.

SEYFRIED JR. W. E., CHEN X. & CHAN L.-H. 1998. Trace element mobility and lithium isotope exchange during hydrothermal alteration of seafloor weathered basalt: an experimental study at 350°C, 500bars. *Geochimica et Cosmochimica Acta* **62**, 949-960.

SHERVAIS J. W. 1982. Ti-V plots and the petrogenesis of modern and ophiolitic lavas. *Earth and Planetary Science Letters* **59**, 101-118.

SONG S., YANG J., LIOU J. G., WU C., SHI R. & XU Z. 2003. Petrology, geochemistry and isotopic ages of eclogites from the Dulan UHPM Terrane, the North Qzi dam, NW China. *Lithos* **70**, 195-211.

SONG S., ZHANG L., NIU Y., SU L., SONG B. & LIU D. 2006. Evolution from Oceanic Subduction to Continental Collision: a Case Study from the Northern Tibetan Plateau Based on Geochemical and Geochronological Data. *Journal of Petrology* **47**, 435-455.

SPANDLER C., HERMANN J., ARCULUS R. & MAVROGENES J. 2004. Geochemical heterogeneity and element mobility in deeply subducted oceanic crust; insights from high-pressure mafic rocks from New Caledonia. *Chemical Geology* **206**, 21-42.

STEIN M. & HOFMANN A. W. 1994. Mantle plumes and episodic crustal growth. *Nature* **372**, 63-68.

STERN R. A., SYME E. C. & LUCAS S. B. 1995. Geochemistry of 1.9 Ga MORB- and OIB-like basalts from the Amisk collage, Flin Flon Belt, Canada: Evidence for an intra-oceanic origin. *Geochimica et Cosmochimica Acta* **59**, 3131-3154.

STERN R. J. 2005. Evidence from ophiolites, blueschists, and ultrahigh-pressure metamorphic terrances that the modern episode of subduction tectonics began in Neoproterozoic time. *Geology* **33**, 557-560

STOSCH H.-G. & LUGMAIR G. W. 1990. Geochemistry and evolution of MORB-type eclogites from the Munchberg Massif, sourthern Germany. *Earth and Planetary Science Letters* **99**, 230-249.

SUN S.-S. 1982. Chemical composition and origin of the earth's primitive mantle. *Geochimica et Cosmochimica Acta* **46**, 179-192.

SUN S.-S. & MCDONOUGH W. F. eds. 1989. *Chemical and isotopic systematics of oceanic basalts: implications for mantle compostion and processes*. Magmatism in the Ocean Basins **42**. Geological Society Special Publication.

SUN S.-S. & NESBITT R. W. 1977. Chemical Heterogeneity of the Archaean mantle, composition of the Earth and mantle evolution. *Earth and Planetary Science Letters* **35**, 429-448.

SUN S.-S. & NESBITT R. W. 1979. Geochemical characteristics of mid-ocean ridge basalts. *Earth and Planetary Science Letters* **44**, 119-138.

TRIBUZIO R., MESSIGA B., VANNUCCI R. & BOTTAZZI P. 1996. Rare earth element redistribution during high-pressure low-temperature metamorphism in ophiolitic Fe-gabbros (Liguria, northwestern Italy): Implications for light REE mobility in subduction zones. *Geology* **24**, 711-714.

TURCOTTE D. L. 1980. On the Thermal Evolution of the Earth. *Earth and Planetary Science Letters* **48**, 53-58.

VOLODICHEV O. I., SLABUNOV A. I., BIBIKOVA E. V., KONILOV A. N. & KUZENKO T. I. 2004. Archean Eclogites in the Belomorian Mobile Belt, Baltic Shield. *Petrology* **12**, 609-631.

WADE B. P., BAROVICH K. M., HAND M., SCRIMGEOUR I. R. & CLOSE D. F. 2006. Evidence for Early Mesoproterozoic Arc Magmatism in the Musgrave Block, Central Australia: Implications for Proterozoic Crustal Growth and Tectonic Reconstruction of Australia. *The Journal of Geology* **114**, 43-63.

WINCHESTER J. A. & FLOYD R. A. 1976. Geochemical Magma Type Discrimination: application to altered and metamorphosed basic igneous rocks. *Earth and Planetary Science Letters* **28**, 459-469.

YANG J., WU C., ZHANG J., SHI R., MENG F., WOODEN J. & YANG H.-Y. 2006. Protolith of eclogites in the north Qaidam and Altun UHP terrane, NW China: Earlier oceanic crust? *Journal of Asian Earth Sciences* **28**, 185-204.

ZHANG G., SONG S., ZHANG L. & NIU Y. 2008. The subducted oceanic crust within continental-type UHPmetamorphic belt in the North Qaidam, NW China: Evidence from petrology, geochemistry and geochonology. *Lithos* **104**, 99-118.

ZHANG J., ZHANG Z., XU Z., YANG J. & CUI J. 2001. Petrology and geochronology of eclogites from the western segment of the Altyn Tagh, northwestern China. *Lithos* **56**, 187-206.

ZHANG L., AI Y., LI X., RUBATTO D., SONG B., WILLIAMS S., SONG S., ELLIS D. & LIOU J. G. 2007. Triasic collision of western Tainshan orogenic belt, China: Evidence from SHRIMP U-Pb dating of zircon from HP/UHP eclogitic rocks. *Lithos* **96**, 266-280.

10. Tables

Table 1 - Major and trace element compositions of the Usagaran eclogites, mafic rocks and pelites

Rock Type	Eclogite									Mafic						Pelite					Mafic (ALS)	
Sample Number	T01-40	T06-08	T06-10	T06-11	T06-16	T07-06	T07-11	T07-16	T07-24	T06-39	T07-53	T07-54	T07-55	T07-56	T07-57	T01-05	T06-07	T06-22	T06-25	T06-27	T06-38	T06-39
SiO_2	47.5	50.4	50.1	48.6	49	52.1	50.9	61.3	48	52.5	52.7	51.8	53.1	51.9	52.2	55.9	35.9	60.1	55.3	54.3	51.6	53
TiO_2	1.7	1.405	1.305	1.555	1.45	0.595	1.165	0.44	0.895	0.48	0.505	0.51	0.67	0.495	0.6	1.695	1.17	1.07	1.88	1.405	1.07	0.53
Al_2O_3	12.7	13.4	13.4	15.8	13.6	14.4	14.4	7.67	14.2	5.95	6.33	6.31	8.3	6.08	7.84	25.6	19.7	17.1	26.4	24.2	13.85	6.21
Fe_2O_3	17.3	15.5	14.6	14.6	14.1	10.9	14.6	9.01	14.1	11.7	11.4	11.6	11.8	11.6	11.5	4.66	11.8	9.69	6.42	12	14.35	11.6
MnO	0.28	0.23	0.21	0.31	0.11	0.18	0.23	0.37	0.45	0.25	0.2	0.2	0.18	0.19	0.19	0.06	0.03	0.11	0.08	0.12	0.23	0.21
MgO	5.47	5.89	5.69	4.46	5.9	6.74	5.63	13.8	7.71	16.1	15.1	14.8	12.6	15.2	12.9	1.83	17.1	2.61	2.01	3.67	5.91	16.1
CaO	12.4	11.1	10.5	10.9	8.74	11.5	10.8	5.59	11.7	9.51	10.3	10.5	10.1	10.2	10.1	2.84	2.46	3.65	2.24	2.24	10.35	9.53
Na_2O	2.24	2.25	2.78	2.42	3.91	2.76	2.54	0.46	2.46	1.5	1.47	1.71	2	1.49	2	2.33	0.19	2.96	1.79	0.6	2.05	1.47
K_2O	0.05	0.1	0.19	0.17	0.76	0.15	0.09	0.11	0.24	0.37	0.36	0.51	0.56	0.37	0.51	1.16	0.57	1.85	1.37	1.56	0.36	0.34
P_2O_5	0.23	0.09	0.09	0.16	0.1	0.05	-	0.06	0.08	0.04	0.04	0.05	0.07	0.06	0.05	0.18	0.09	0.13	0.2	0.24	0.14	0.1
LOI	0.18	-0.27	0.52	0.47	0.8	0.69	0.16	0.3	0.8	0.27	0.19	0.54	-0.04	0.28	0.1	-	8.62	1	0.86	0.36	-	-
Total	100.05	100.10	99.39	99.45	98.47	100.07	100.52	99.11	100.64	98.67	98.60	98.53	99.34	97.87	97.99	96.26	97.63	100.27	98.55	100.70	99.91	99.09
Mg#	0.2142	0.2468	0.2515	0.2085	0.2651	0.3477	0.2495	0.5691	0.3204	0.5426	0.5332	0.5238	0.4793	0.5305	0.4917	-	-	-	-	-	0.2620	0.5448
Sr	105	55	75	110	155	105	65	9.5	155	155	145	125	185	135	195	190	32	265	120	85	135	149.5
Cs	-	-	-	-	-	-	-	-	0.1	0.3	0.3	0.2	0.4	0.3	0.4	0.7	0.2	2.7	1.5	1.3	1	0.25
Rb	1.4	4.1	2.5	1.8	2.8	1.4	0.9	1.1	1.2	10	9.5	6	14.5	9	14	31	15.5	70	40	70	11.1	9.4
Ba	10	55	210	700	150	60	45	45	55	145	130	160	210	155	270	600	130	650	600	600	300	136.5
Th	0.6	0.3	0.5	0.7	0.4	0.4	0.3	0.2	0.4	1.3	1.2	1.1	1.7	1.1	1.5	13	0.6	8	10.5	15	0.89	0.97
U	0.2	0.4	0.2	0.5	0.3		0.2	0.2	0.1	0.2	0.2	0.2	0.3	0.2	0.4	2.1	1.5	1.3	1.3	1.7	0.1	0.18
Nb	7.5	6	6	8	8	2.5	6	0.5	4	-	-	0.5	1.5	-	1	7	3.5	1.5	2	3	3.5	2.4
Zr	95	80	75	85	85	50	70	50	55	45	45	45	70	45	60	850	65	170	265	220	49	22
Hf	3	2	2	2	2	2	2	1	2	1	1	1	2	1	1	21	2	4	7	6	1.8	0.8
Y	31.5	25	25	38.5	24	19.5	19.5	11.5	21	8	8.5	8.5	10.5	8.5	10	26.5	2.7	26	32.5	38.5	22	8.2
Co	75	75	70	75	50	70	75	85	75	90	90	80	75	85	75	65	39.5	47.5	75	55	76.6	113
Cr	135	155	195	375	145	95	145	2000	400	3100	2900	2800	2200	2700	2300	650	550	385	650	500	150	3460
Ni	55	85	85	110	95	80	75	550	70	600	500	500	415	500	430	175	160	70	240	80	92	592
V	430	375	350	340	360	215	300	130	310	180	200	200	200	195	200	355	260	235	445	390	332	102
Zn	135	110	100	135	60	95	100	210	255	85	75	80	80	75	85	105	47.5	100	37.5	115	114	81
Sc	45	45	45	40	45	45	40	20	50	30	35	35	30	30	30	45	35	30	60	50	-	-
La	5.5	4	8	15	10.5	8	2.5	4.5	5	8	7.5	8.5	10.5	7	9	36.5	1.5	25.5	25.5	30.5	8.6	8.5
Ce	14	11	18	39	20.5	19	6	14	14.5	16.5	15.5	18	22	15	19.5	85	3	47.5	50	70	16.7	16.7
Pr	2.1	1.7	2.5	5.5	2.4	2.6	1.2	2	2.1	2	1.95	2.1	2.7	1.85	2.4	8.5	0.4	5.5	6.5	8.5	1.93	1.81
Nd	11	9	11.5	23.5	10.5	11.5	7	9	10	8.5	8	9	11.5	8	10	34	1.85	23	26	33	9.2	7.5
Sm	3.5	2.9	3.3	5.5	2.9	3	2.6	2.1	2.7	1.9	1.95	2	2.6	1.85	2.3	7	0.54	5	5.5	6.5	2.59	1.64
Eu	1.15	1.1	1.2	1.55	1.3	1	1.05	0.56	0.84	0.6	0.6	0.68	0.8	0.6	0.72	2	0.18	1.6	1.35	1.45	0.89	0.5
Gd	4.4	3.7	3.8	6	3.4	3.2	3.4	2	3.1	1.7	1.85	1.9	2.3	1.85	2.1	6	0.55	5.5	4.6	6	3.24	1.72
Tb	0.8	0.68	0.68	1	0.62	0.58	0.58	0.34	0.56	0.28	0.3	0.3	0.36	0.28	0.34	0.98	0.1	0.88	0.84	1.05	0.61	0.28
Dy	6	4.7	4.8	7	4.4	3.9	4	2.2	4	1.75	1.85	1.85	2.3	1.75	2.1	6	0.56	5.5	6	7.5	3.65	1.55
Ho	1.15	0.92	0.92	1.35	0.88	0.72	0.72	0.42	0.76	0.32	0.32	0.32	0.4	0.32	0.38	1.05	0.1	0.94	1.25	1.4	0.79	0.3
Er	3.5	2.8	2.8	4.2	2.7	2.2	2.1	1.25	2.4	0.9	1	0.95	1.15	0.95	1.1	3.1	0.4	2.7	3.9	4.2	2.36	0.87
Tm	0.55	0.4	0.4	0.65	0.4	0.3	0.3	0.2	0.35	0.15	0.15	0.15	0.15	0.1	0.15	0.45	0.05	0.4	0.55	0.6	0.32	0.11
Yb	3.5	2.8	2.7	4.4	2.8	2.1	2	1.2	2.4	0.85	0.9	0.85	1.1	0.85	1	3	0.55	2.6	3.9	4.1	2.25	0.77
Lu	0.52	0.42	0.4	0.64	0.4	0.3	0.28	0.16	0.32	0.12	0.12	0.12	0.16	0.12	0.14	0.44	0.1	0.36	0.54	0.58	0.32	0.1
Total REE	57.67	46.12	61	115.29	63.7	58.4	33.73	39.93	49.03	43.57	41.99	46.72	58.02	40.52	51.23	194.02	9.88	126.98	136.43	175.38	53.45	42.35
$(La/Sm)_N$	1.014	0.890	1.565	1.761	2.337	1.722	0.621	1.383	1.195	2.718	2.483	2.744	2.607	2.443	2.526	-	-	-	-	-	2.144	3.346
$(La/Yb)_N$	1.127	1.025	2.125	2.445	2.690	2.733	0.897	2.690	1.494	6.751	5.977	7.173	6.847	5.907	6.456	-	-	-	-	-	2.742	7.918

Table 2 – Sm-Nd Isotopic compositions of the Usagaran eclogites, mafic rocks and pelites

	Sample	147Sm/144Nd	143Nd/144Nd	143Nd/144Nd Initial	εNd (2.0 Ga)	εNd (Now)
Eclogite	T01-40	0.190942	0.512685	0.510171	2.4	0.9
	T06-08	0.199970	0.512702	0.510070	0.4	1.3
	T06-11	0.137436	0.511770	0.509961	-1.7	-16.9
	T07-06	0.151024	0.511837	0.509848	-3.9	-15.6
	T07-11	0.231633	0.513077	0.510027	-0.4	8.6
Mafic	T07-53	0.137294	0.511662	0.509854	-3.8	-19.0
	T07-55	0.133800	0.511613	0.509851	-3.9	-20.0
	T07-56	0.137322	0.511649	0.509841	-4.1	-19.3
Pelite	T01-05	0.115246	0.511379	0.509861	-3.7	-24.6
	T06-22	0.131352	0.511321	0.509591	-9.0	-25.7

Table 3 – Sm-Nd Isotopic compositions of the Tanzanian Craton, Usagaran eclogites and pelites (Möller *et al.*, 1998)

	Sample	147Sm/144Nd	143Nd/144Nd	$^{143}Nd/^{144}Nd_{(0)}$	εNd (2.0 Ga)	εNd (2.7 Ga)	εNd (Now)
Eclogite	T69G Mb (M)	0.184900	0.512534	0.510100	1.0	-	-2.0
Pelite	T69G Mp (M)	0.122300	0.511297	0.509687	-7.1	-	-26.2
	T70G (M)	0.111900	0.511175	0.509702	-6.8	-	-28.5
	A167-16 (M)	0.161700	0.511482	0.509353	-13.7	-	-22.6
Tanzanian Craton	T71-1 (M)	0.122900	0.511313	0.509287	-	-14.9	-25.8
	A159-1 a (M)	0.111600	0.511153	0.509313	-	-14.4	-29.0
	A159-1 b (M)	0.112700	0.511181	0.509323	-	-14.2	-28.4

Table 4 - Comparison among eclogites from Usagaran Belt and other eclogites with similar tectonic settings. Dulan Belt Eclogite data from Song *et al.*, (2003), Alpine External Crystalline Massifs data from Paquette *et al.* (1989). # from Möller *et al.*, (1995); ^ from Collins *et al.*, (2004); * from Brick, unpublished data.

	Usagaran Eclogite, Tanzania	Dulan Belt Eclogite, China	Alpine External Crystalline Massifs (Aiguilles Rouges, Belledonne and Argentera)
Age of Eclogitization	• 1999.1 ± 2 Ma from monazite in pelite by U-Pb dating^ • 1999 ± 2 Ma from zircons in eclogite by U-Pb dating#	• NDB: 459 ± 2.6 Ma by Sm-Nd dating • SDB: 497 ± 87 Ma by Sm-Nd dating	• Two eclogitic metamorphic events: Argentera Massif at 424 Ma & Belledonne Massif at 395 Ma by U-Pb dating • Younger one probably correlated with Aiguilles Rouges Massif
Eclogite outcrop appearance	Eclogites occur in the garnet amphibolites, together with metapelites and felsic gneisses in the Isimani Suite^	• NDB: Eclogites occur as lenses or blocks in granitic and aluminum-rich pelitic gneisses • SDB: Eclogites occur as lensoid blocks within both granitic and pelitic gneisses and marble	• Aiguilles Rouges Massif: Eclogite preserved in the cores of basic lenses intercalated with amphibolite gneisses • Belledonne and Argentera Massifs: Eclogites occur as relictual bodies surrounded by amphibolitic and migmatitic gneisses
Peak Metamorphic Condition	• 750 – 800°C, ~ 18 kbar# • Up to 800°C, ~ 18 kbar*	• NDB: 687°C, 32 kbar • SDB: 729 – 768 °C, 29 – 33 kbar	• Aiguilles Rouges Massif: 780°C, 11 kbar • Argentera Massif: 700°C, 14 kbar
Protolith(s)	• Plume-type MORB# • E - MORB	• NDB: N-MORB and E-MORB • SDB: Island arc	Both N-type and E-type MORB
Sm-Nd Isotopic Compositions	• εNd = 1.25 at 2.2 Ga# • εNd = -3.95 – 2.38 at 2.0 Ga	• NDB: εNd = -0.8 ± 1.1 at 458 Ma and 1.4 ± 0.6 in 459 Ma • SDB: εNd = 1.7 ± 1.7 at 497 Ma, but doubt	Initial εNd = 6 – 8
REE patterns & significances	Contaminations in some eclogitic samples	Protolith derived from a slightly enriched to depleted mantle, or contaminated by crustal compositions	Slightly crustal influence is apparent in the LILE distribution pattern

11. Figures

Figure 1

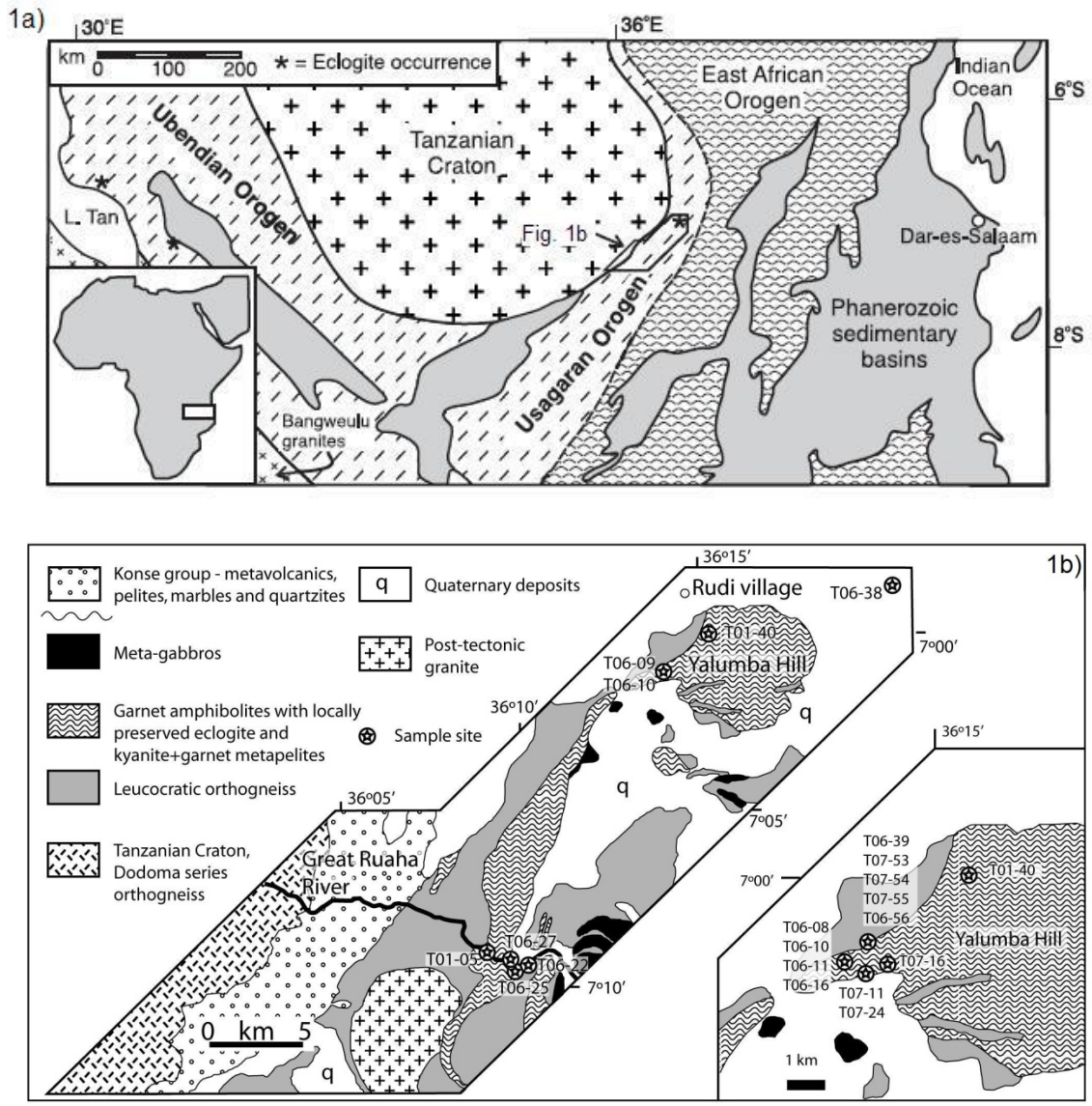

Figure 2

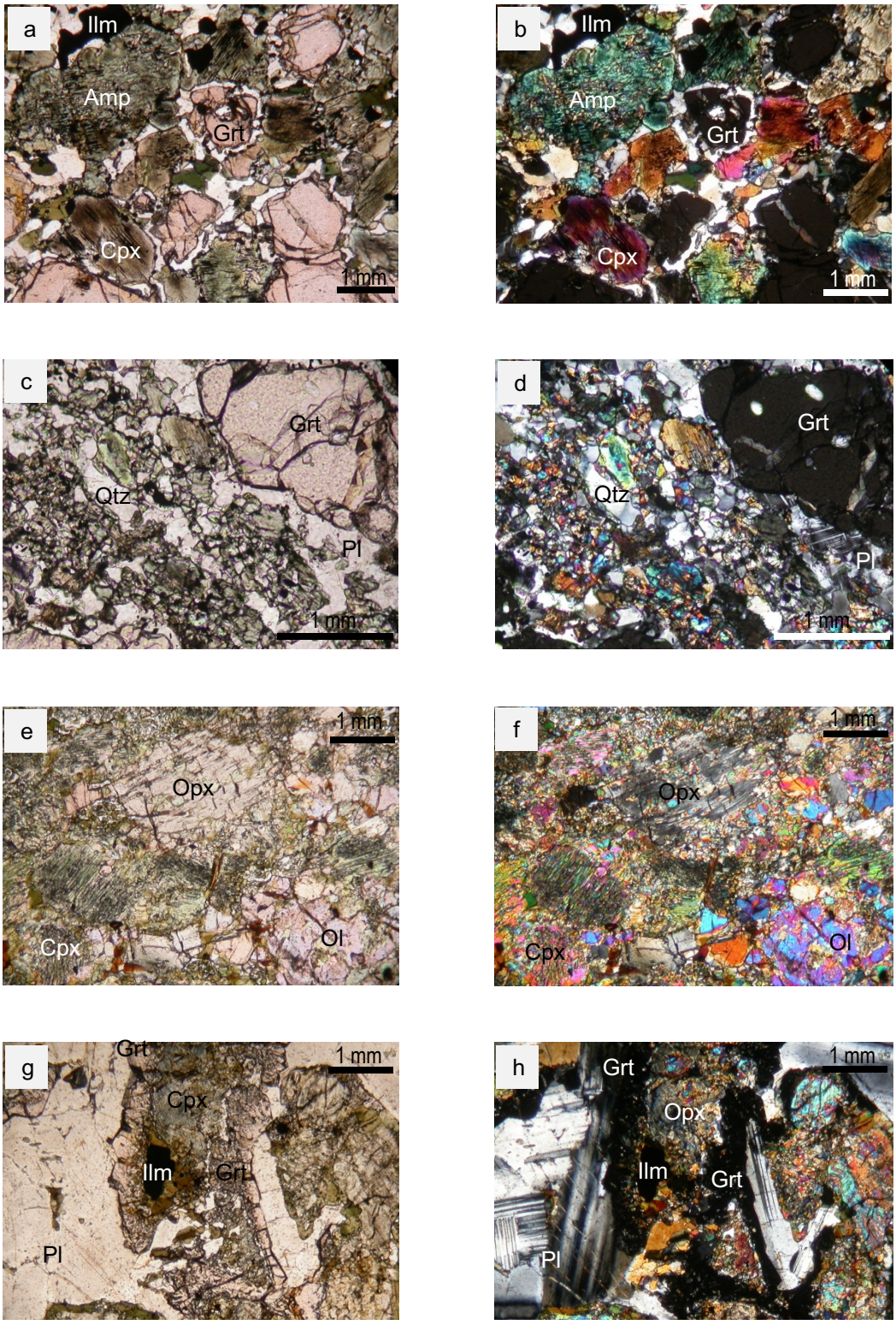
a
Ilm
Amp
Grt
Cpx
1 mm
b
Ilm
Amp
Grt
Cpx
1 mm
c
Grt
Qtz
Pl
1 mm
d
Grt
Qtz
Pl
1 mm
e
1 mm
Opx
Cpx
Ol
f
1 mm
Opx
Cpx
Ol
g
Grt
1 mm
Cpx
Ilm
Grt
Pl
h
Grt
1 mm
Opx
Ilm
Grt
Pl

Figure 3

a)

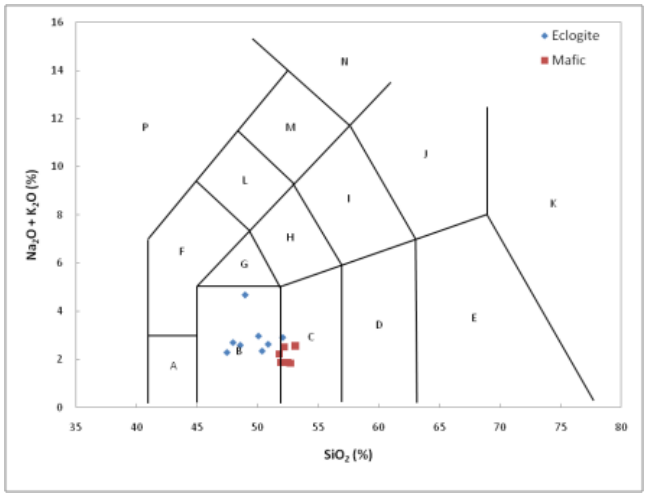

A: Picrobasalt, B: Basalt, C: Basaltic andesite, D: Andesite, E: Dacite, F: Tephrite & Basanite, G: Trachybasalt, H: Basaltic trachyandesite, I: Trachyandesite, J: Trachyte & Trachydacite, K: Rhyolite, L: Phonotephrite; M: Tephriphonolite; N: Phonolite, P: Foidite

b)

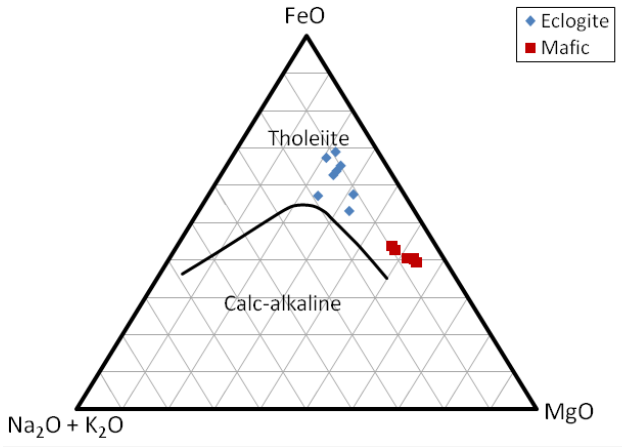

c)

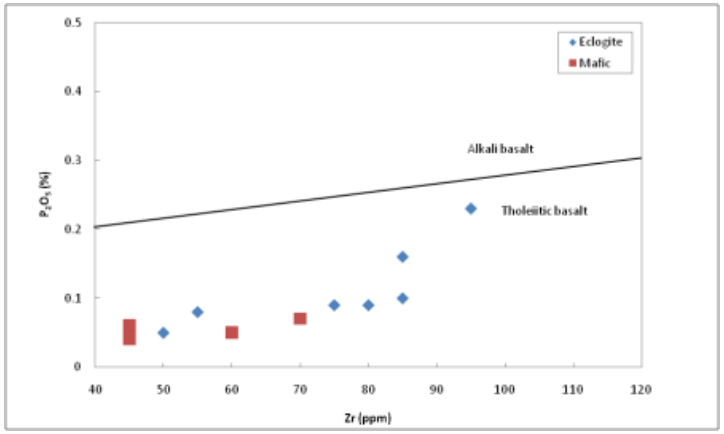

d)

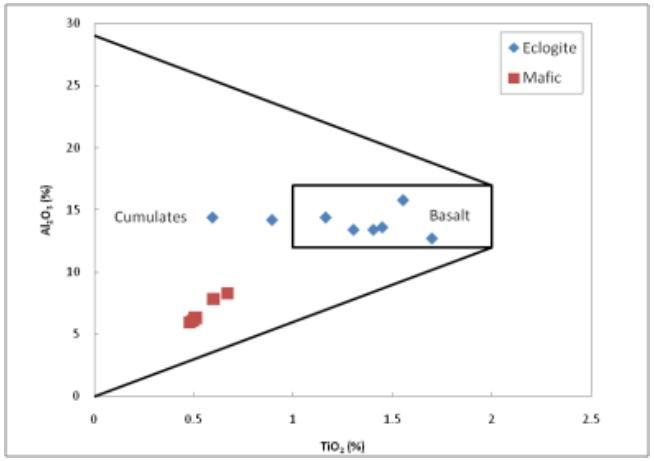

Figure 4

a)

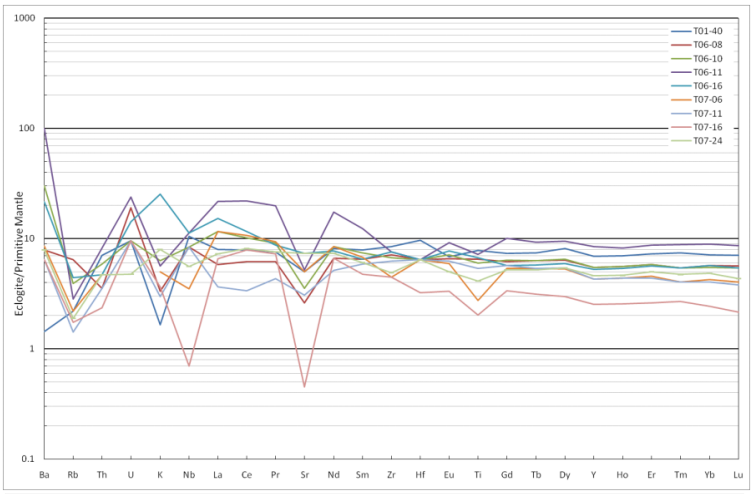
Eclogite/Primitive Mantle
1000
100
10
1
0.1
Ba Rb Th U K Nb La Ce Pr Sr Nd Sm Zr Hf Eu Ti Gd Tb Dy Y Ho Er Tm Yb Lu
T01-40
T06-08
T06-10
T06-11
T06-16
T07-06
T07-11
T07-16
T07-24

b)

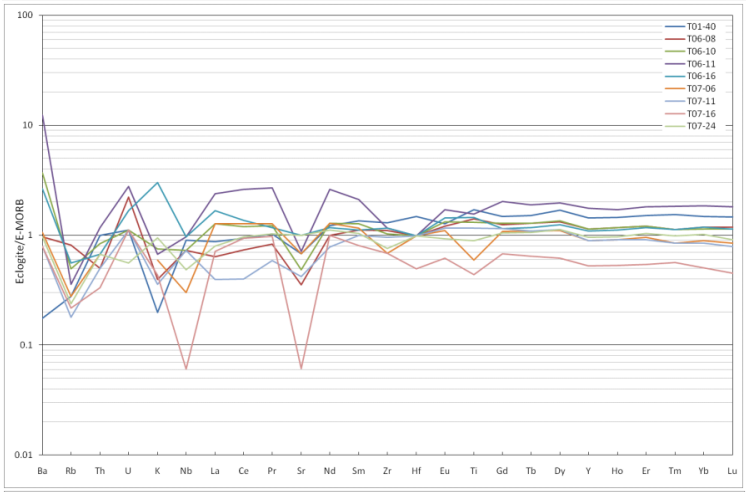
Eclogite/E-MORB
100
10
1
0.1
0.01
Ba Rb Th U K Nb La Ce Pr Sr Nd Sm Zr Hf Eu Ti Gd Tb Dy Y Ho Er Tm Yb Lu
T01-40
T06-08
T06-10
T06-11
T06-16
T07-06
T07-11
T07-16
T07-24

c)

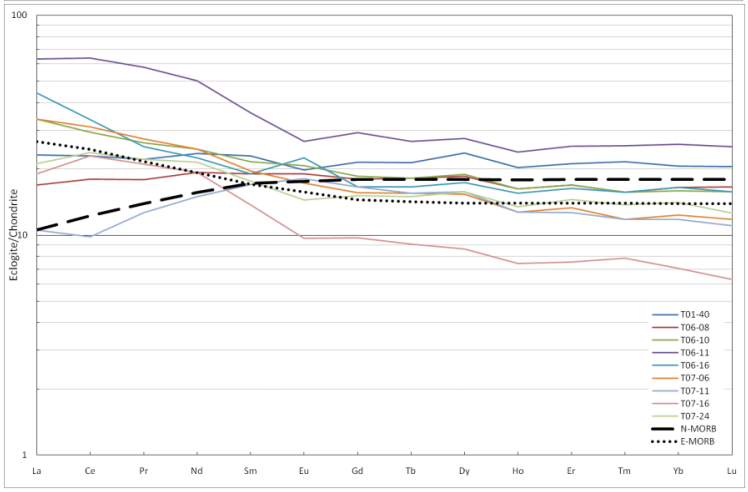
Eclogite/Chondrite
100
10
1
La Ce Pr Nd Sm Eu Gd Tb Dy Ho Er Tm Yb Lu
T01-40
T06-08
T06-10
T06-11
T06-16
T07-06
T07-11
T07-16
T07-24
N-MORB
E-MORB

Figure 5

a)

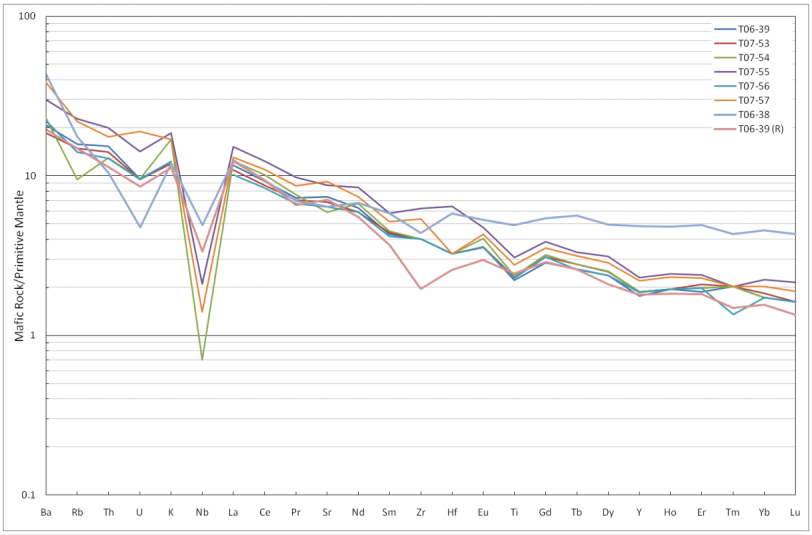
100
10
1
0.1
Mafic Rock/Primitive Mantle
Ba Rb Th U K Nb La Ce Pr Sr Nd Sm Zr Hf Eu Ti Gd Tb Dy Y Ho Er Tm Yb Lu
T06-39
T07-53
T07-54
T07-55
T07-56
T07-57
T06-38
T06-39 (R)

b)

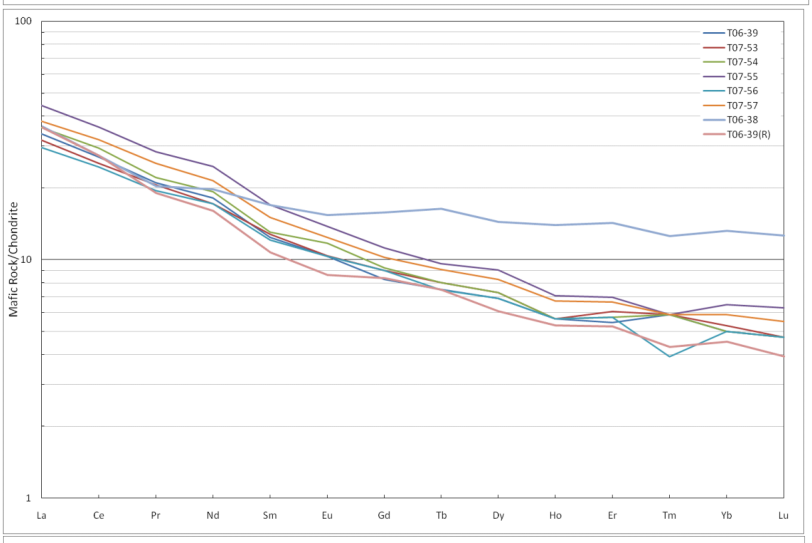
100
10
1
Mafic Rock/Chondrite
La Ce Pr Nd Sm Eu Gd Tb Dy Ho Er Tm Yb Lu
T06-39
T07-53
T07-54
T07-55
T07-56
T07-57
T06-38
T06-39(R)

c)

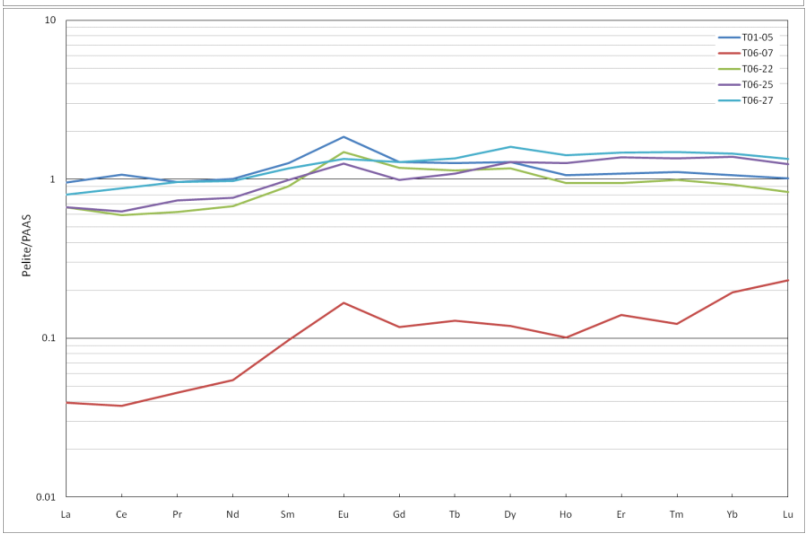
10
1
0.1
0.01
Pelite/PAAS
La Ce Pr Nd Sm Eu Gd Tb Dy Ho Er Tm Yb Lu
T01-05
T06-07
T06-22
T06-25
T06-27

Figure 6

a)

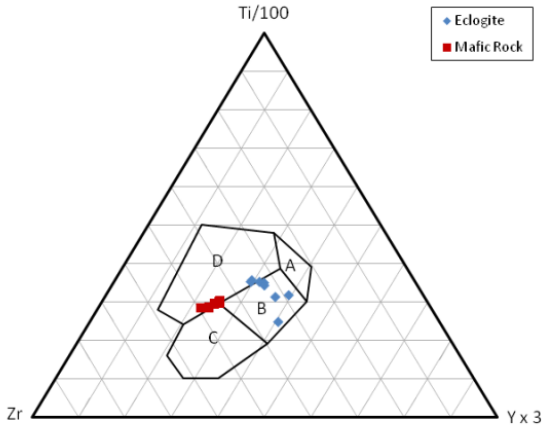

A: Island-arc tholeiites; B: MORB, island-arc tholeiites & calc-alkali basalts;
C: Calc-alkali basalts; D: Within-plate basalts

b)

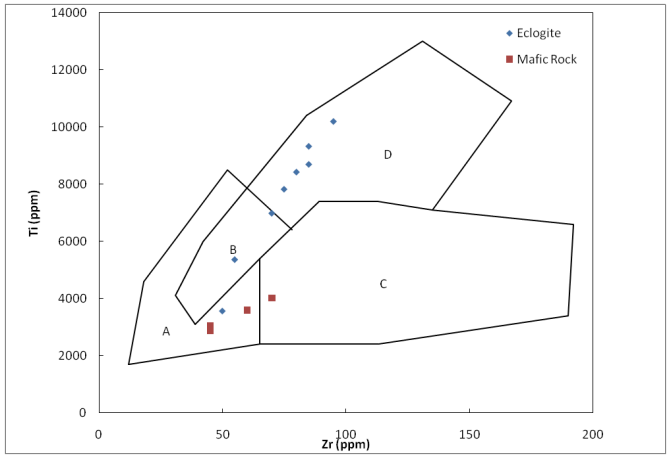

A: Island-arc tholeiites; B: MORB, calc-alkali basalts and island-arc thoeiites;
C: calc-alkali basalt; D: MORB

c)

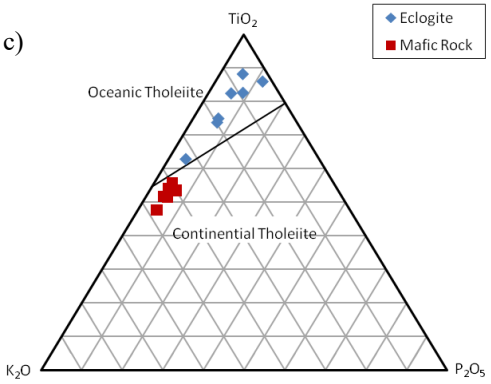

d)

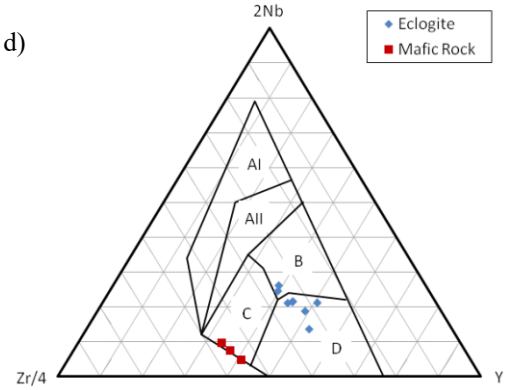

AI: Within-plate alkali basalts; AII: Within-plate basalts and within-plate tholeiites;
B: E-type MORB; C: within-plate tholeiites and volcanic-arc basalts;
D: N-type MORB and volcanic-arc basalts

e)

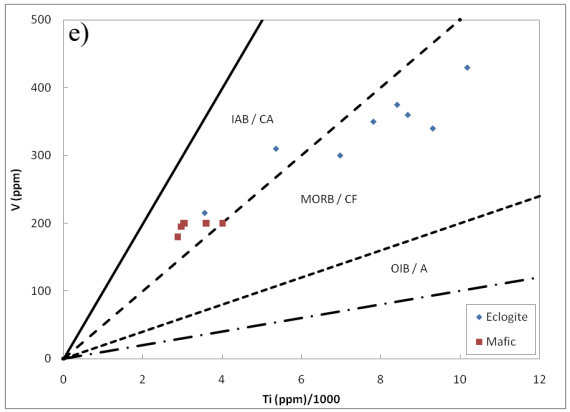

Figure 7

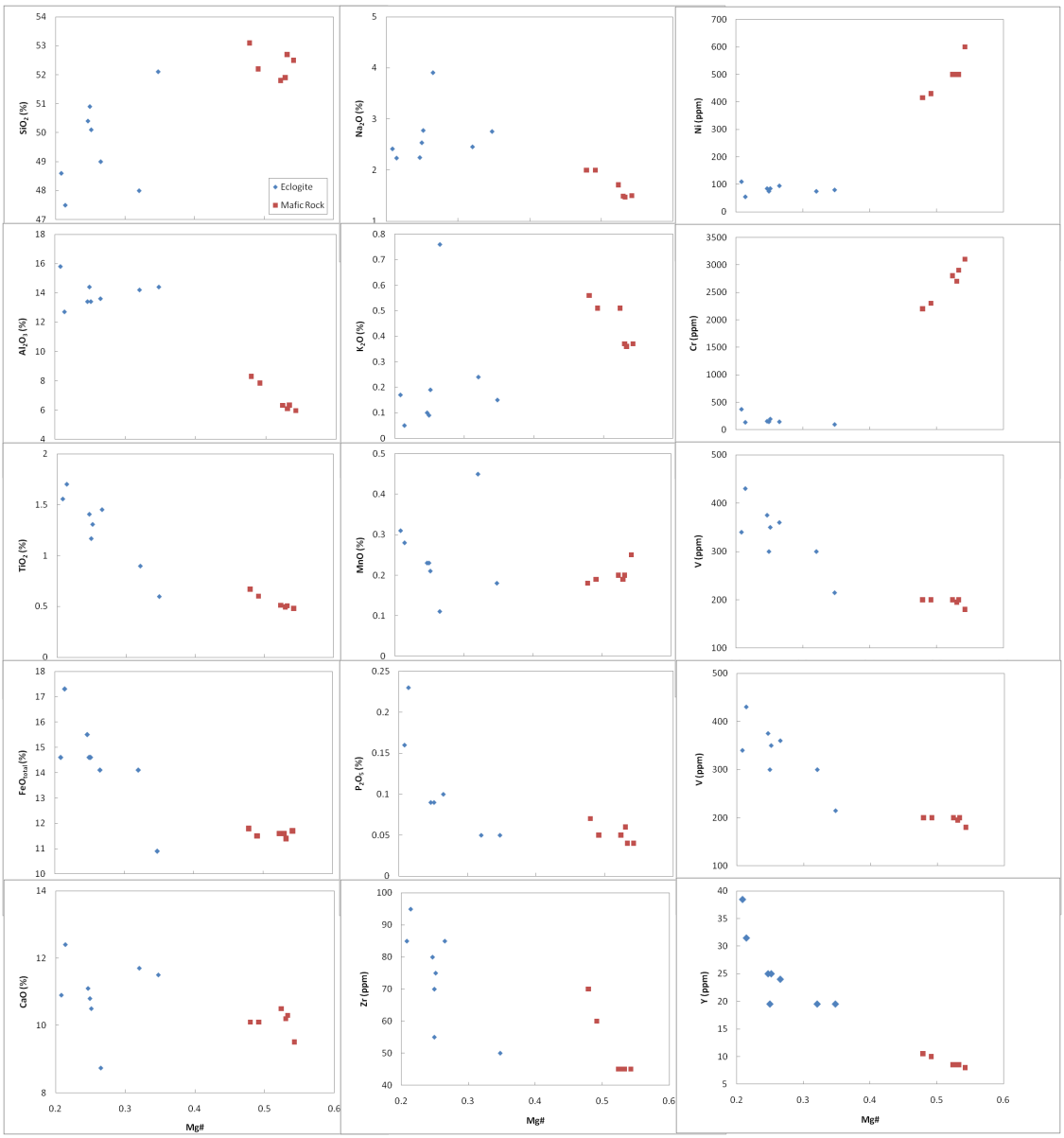
SiO2 (%)
Na2O (%)
Ni (ppm)
Al2O3 (%)
K2O (%)
Cr (ppm)
TiO2 (%)
MnO (%)
V (ppm)
FeOTotal (%)
P2O5 (%)
V (ppm)
CaO (%)
Zr (ppm)
Y (ppm)
Mg#
Mg#
Mg#
Eclogite
Mafic Rock

Figure 8

a)

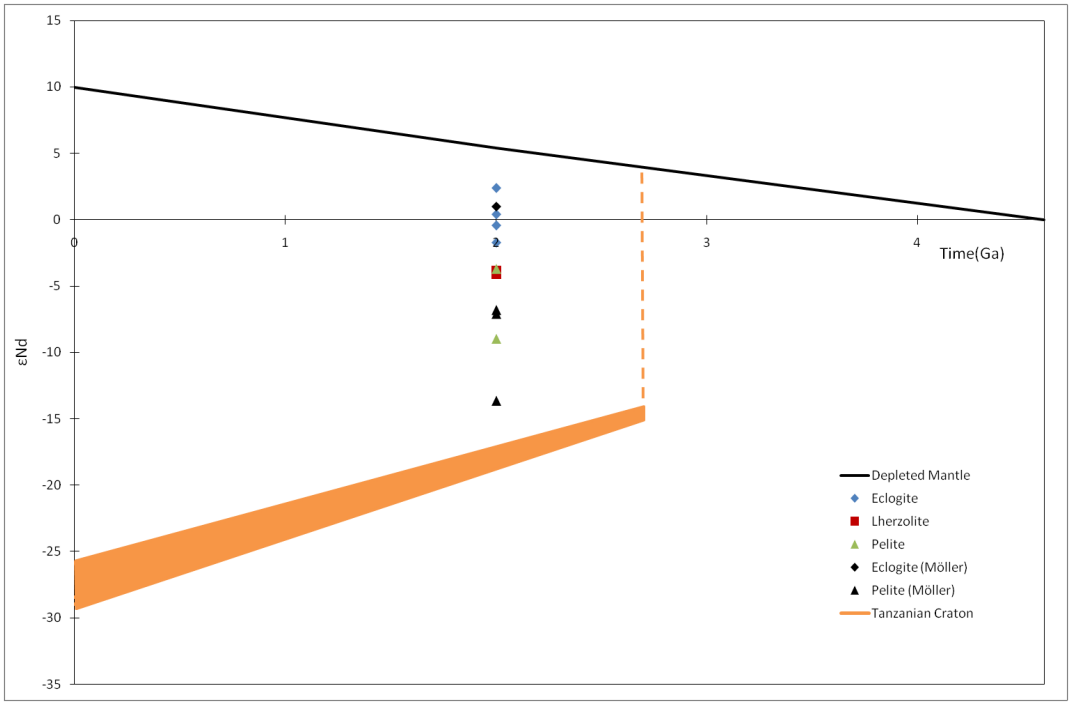
15
10
5
0
-5
-10
-15
-20
-25
-30
-35
εNd
0
1
2
3
4
Time(Ga)
Depleted Mantle
Eclogite
Lherzolite
Pelite
Eclogite (Möller)
Pelite (Möller)
Tanzanian Craton

b)

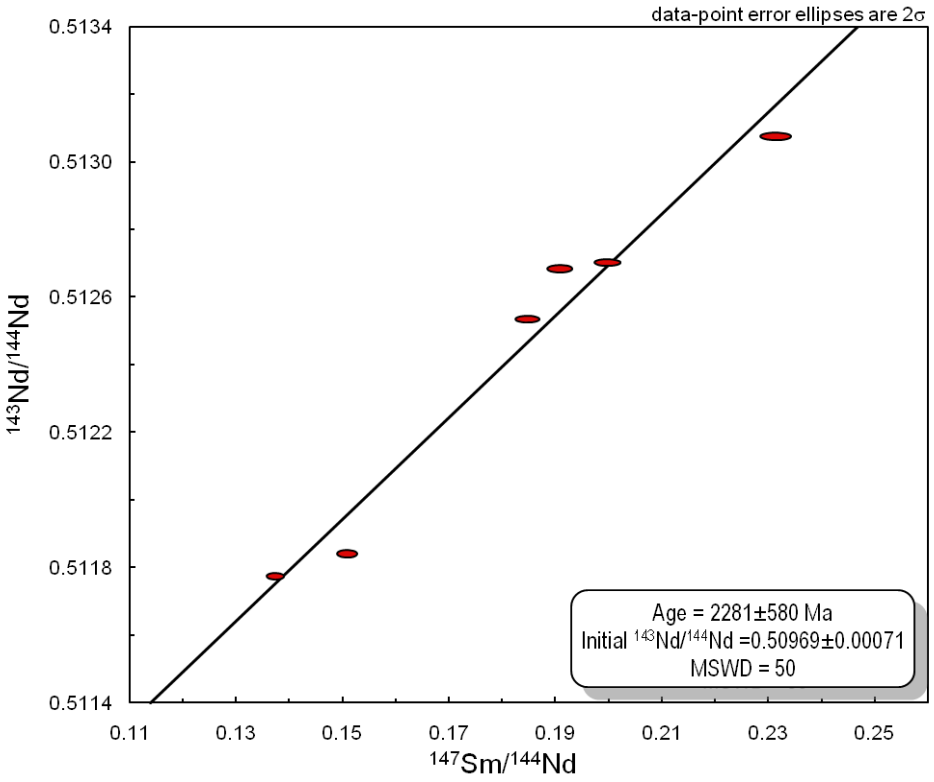
data-point error ellipses are 2σ
0.5134
0.5130
0.5126
0.5122
0.5118
0.5114
143Nd/144Nd
0.11
0.13
0.15
0.17
0.19
0.21
0.23
0.25
147Sm/144Nd
Age = 2281±580 Ma
Initial 143Nd/144Nd =0.50969±0.00071
MSWD = 50

Figure 9

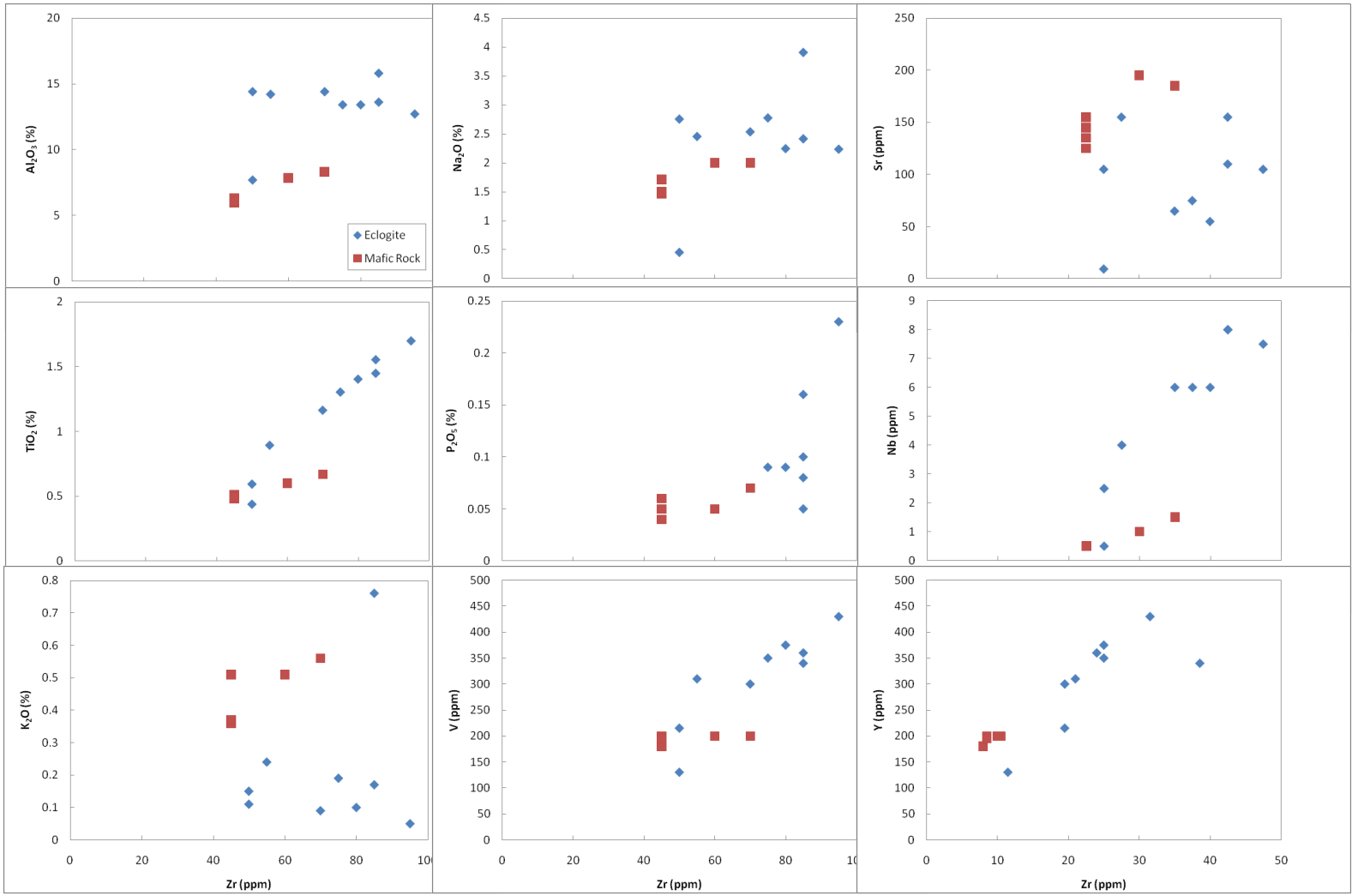
Al2O3 (%)
Eclogite
Mafic Rock
Na2O (%)
Sr (ppm)
TiO2 (%)
P2O5 (%)
Nb (ppm)
K2O (%)
V (ppm)
Y (ppm)
Zr (ppm)
Zr (ppm)
Zr (ppm)

Figure 10

a)

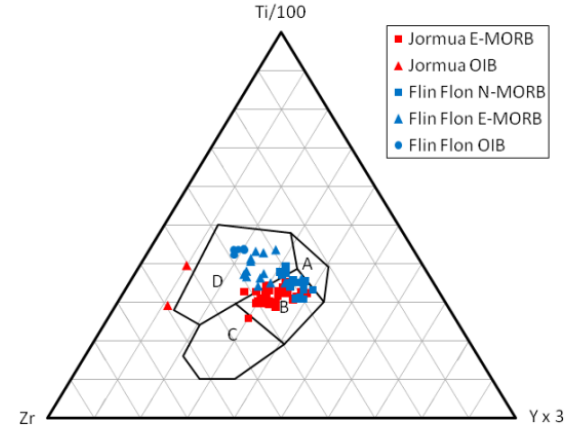

A: Island-arc tholeiites; B: MORB, island-arc tholeiites & calc-alkali basalts;
C: Calc-alkali basalts; D: Within-plate basalts

b)

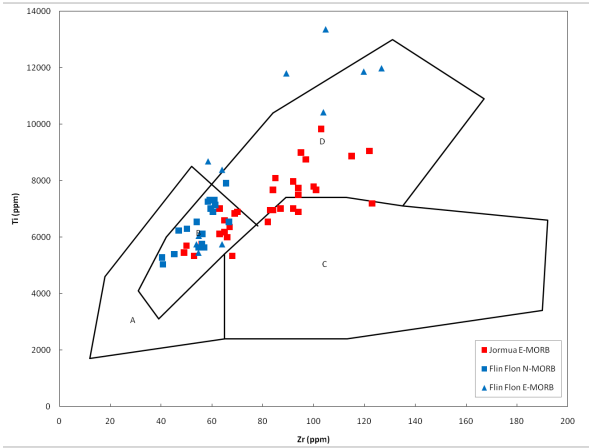

A: Island-arc tholeiites; B: MORB, calc-alkali basalts and island-arc thoeiites;
C: calc-alkali basalt; D: MORB

c)

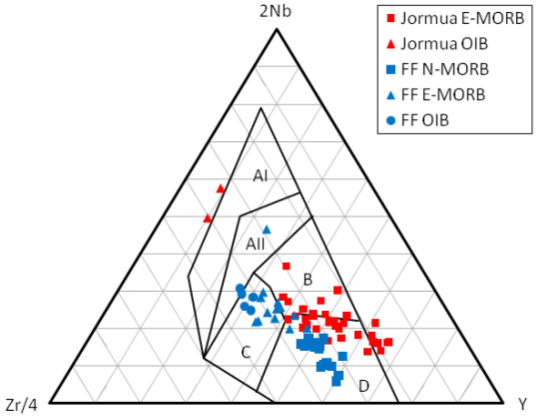

AI: Within-plate alkali basalts; AII: Within-plate basalts and within-plate tholeiites;
B: E-type MORB; C: within-plate tholeiites and volcanic-arc basalts;
D: N-type MORB and volcanic-arc basalts

d)

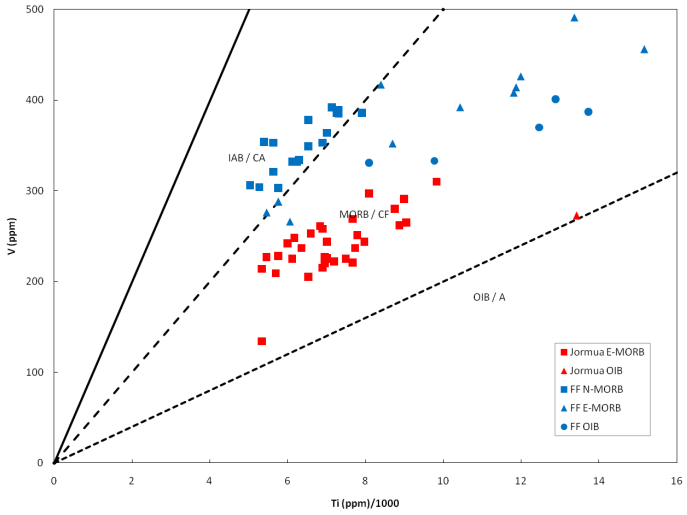

Figure 11

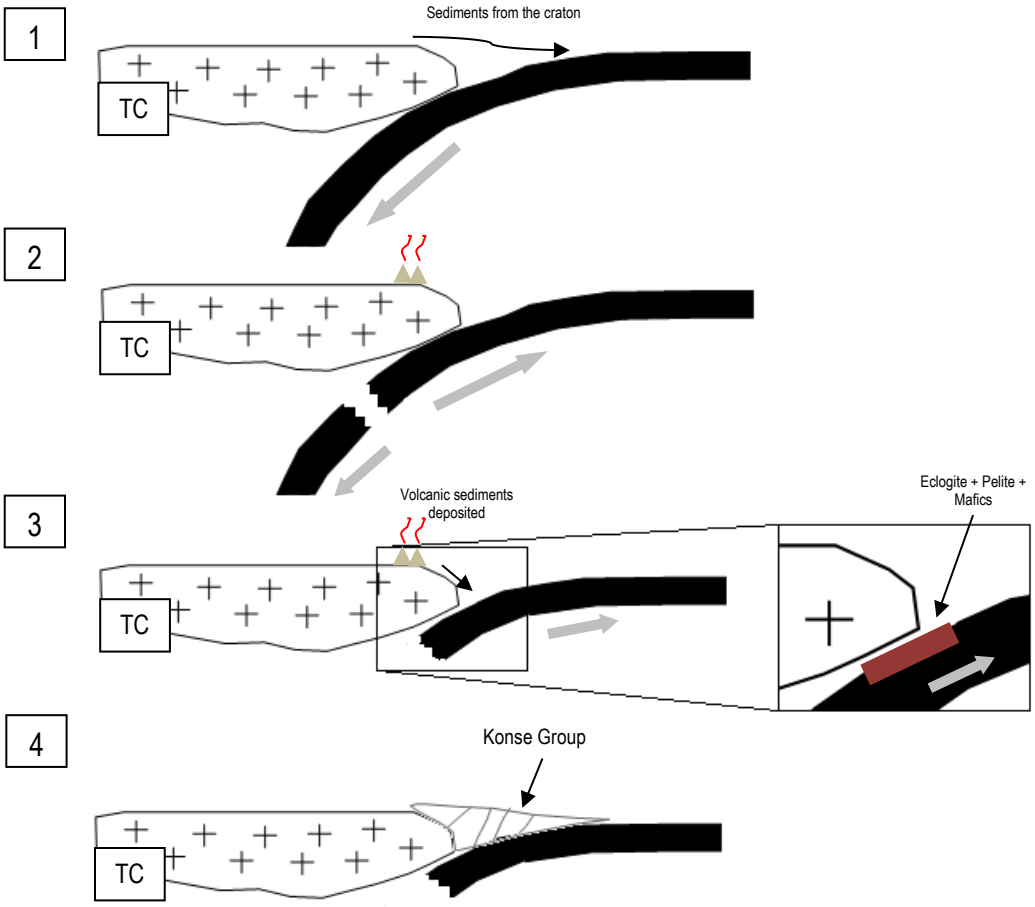
1
Sediments from the craton
TC
2
TC
3
Volcanic sediments deposited
Eclogite + Pelite + Mafics
TC
4
Konse Group
TC

12. Figure captions

Figure 1. (a) Geological map of part of East Africa. Map and lithological subdivisions are after Reddy *et al.*, (2004). (b) Geological map of part of the Usagaran Orogen, Tanzania. Map and lithological subdivision are after Reddy et al. (2004).

Figure 2. a) & b) Photomicrograph of eclogitic sample T01 – 40 under plane polarized light and cross polarized light respectively. c) and d) Photomicrograph of eclogitic sample T06 – 11 under plane polarized light and cross polarized light respectively. e) and f) Photomicrograph of mafic sample T06 – 39 under plane polarized light and cross polarized light respectively. g) and h) Photomicrograph of mafic sample T06 – 38 under plane polarized light and cross polarized light respectively. Abbreviations: Amp= amphibole, Cpx=clinopyroxene, Grt=garnet, Ilm=ilmenite, Opx=orthopyroxene, Pl=plagioclase Qtz=quartz.

Figure 3. a) TAS diagram after Le Maitre *et al.* (1989), as cited in Rollinson (1995). b) AFM diagram classifications for the Usagaran eclogite and mafic rocks. Boundary after Irvine and Baragar (1971), as cited in Rollinson (1995). c) P_2O_5-TiO_2 discrimination diagram (after Winchester and Floyd, 1976). d) $A1_2O_3$- TiO_2 discrimination diagram after Pearce (1983) as cited in Miller and Thöni (1997) and Sassi *et al.* (2004).

Figure 4. a) Primitive mantle normalized spidergram of Usagaran eclogites. b) E-MORB normalized spidergram of Usagaran eclogites. c) Chondrite normalized REE diagram of Usagaran eclogites. Ideal N-MORB and E-MORB are plotted by normalized N-MORB and E-MORB values to chondrite. All normalizing values are from Sun and McDonough (1989).

Figure 5. a) Primitive mantle normalized spidergram of Usagaran mafic rocks. b) Chondrite normalized REE diagram of Usagaran mafic rocks. Normalizing values are from Sun and McDonough (1989). c) PAAS normalized REE diagram of Usagaran pelites. Normalizing values are from McLennan (1989) as cited in Rollinson (1995).

Figure 6. a) and b) Ti-Zr-Y discrimination diagram and Ti-Zr discrimination diagram respectively (after Pearce and Cann, 1973). c) Ti-K-P oxides discrimation dragram (after

Pearce *et al.*, 1975). d) Zr-Nb-Y discrimination diagram (after Meschede, 1986). e) Ti-V discrimination diagram (after Shervais, 1982).

Figure 7. Harker diagrams where all major oxides (except MgO) and some trace elements are plotted against Mg#.

Figure 8. a) εNd evolution diagram of Usagaran eclogite, mafic rocks and pelites. Additional samples from Möller et al. (1998) are included. Orange array represents the εNd evolution path of Tanzanian Craton. Depleted mantle $_{t(0)}$= 0.51315 (Goldstein et al., 1984). b) Sm-Nd errorchron of the Usagaran eclogitic samples calculated using Isoplot (Ludwig, 2008).

Figure 9. Elements that have been used in discrimination diagrams plotted against Zr (after Kullerud *et al.*, 1990).

Figure 10. Classification of the 1.95 Ga Jormua Ophiolite from northeastern Finland (Peltonen *et al.*, 1996) and the 1.9 Ga Flin Flon Belt from Canada (Stern *et al.*, 1995) by discrimination diagrams. a) and b) Ti-Zr-Y discrimination diagram and Ti-Zr discrimination diagram respectively (after Pearce and Cann, 1973). c) Zr-Nb-Y discrimination diagram (after Meschede, 1986). d) Ti-V discrimination diagram (after Shervais, 1982).

Figure 11. Cartoon diagram showin the formation and exhumation of the Usagaran eclogites, mafic and pelite. Grey arrows represent the motion of the plate. Abbrevation: TC = Tanzanian Craton.